

PRIMARY RESEARCH ARTICLE

Ecological forecasting of tree growth: Regional fusion of tree-ring and forest inventory data to quantify drivers and characterize uncertainty

Kelly A. Heilman¹  | Michael C. Dietze²  | Alexis A. Arizpe³  | Jacob Aragon¹ | Andrew Gray^{1,4} | John D. Shaw⁵  | Andrew O. Finley⁶  | Stefan Klesse⁷  | R. Justin DeRose⁸  | Margaret E. K. Evans¹ 

¹Laboratory of Tree Ring Research, University of Arizona, Tucson, Arizona, USA

²Department of Earth & Environment, Boston University, Boston, Massachusetts, USA

³Austrian Academy of Sciences, Gregor Mendel Institute, Vienna, Austria

⁴Western Michigan University Homer Stryker M.D. School of Medicine, Kalamazoo, Michigan, USA

⁵Rocky Mountain Research Station, USDA Forest Service, Ogden, Utah, USA

⁶Department of Forestry, Michigan State University, East Lansing, Michigan, USA

⁷Department of Forest Dynamics, Department of Forest Resources and Management, Swiss Federal Institute for Forest, Snow, and Landscape Research WSL, Birmensdorf, Switzerland

⁸Department of Wildland Resources and Ecology Center, Utah State University, Logan, Utah, USA

Correspondence

Kelly A. Heilman, Laboratory of Tree Ring Research, University of Arizona, Tucson, AZ, USA.
Email: kellyannheilman@gmail.com

Funding information

National Science Foundation, Grant/Award Number: 1458021, 1638577, 1702996, DBI-0735191, DBI-1265383 and DBI-1743442; Division of Environmental Biology, Grant/Award Number: MSB-ECA 1802893

Abstract

Robust ecological forecasting of tree growth under future climate conditions is critical to anticipate future forest carbon storage and flux. Here, we apply three ingredients of ecological forecasting that are key to improving forecast skill: data fusion, confronting model predictions with new data, and partitioning forecast uncertainty. Specifically, we present the first fusion of tree-ring and forest inventory data within a Bayesian state-space model at a multi-site, regional scale, focusing on *Pinus ponderosa* var. *brachyptera* in the southwestern US. Leveraging the complementarity of these two data sources, we parsed the ecological complexity of tree growth into the effects of climate, tree size, stand density, site quality, and their interactions, and quantified uncertainties associated with these effects. New measurements of trees, an ongoing process in forest inventories, were used to confront forecasts of tree diameter with observations, and evaluate alternative tree growth models. We forecasted tree diameter and increment in response to an ensemble of climate change projections, and separated forecast uncertainty into four different causes: initial conditions, parameters, climate drivers, and process error. We found a strong negative effect of fall–spring maximum temperature, and a positive effect of water-year precipitation on tree growth. Furthermore, tree vulnerability to climate stress increases with greater competition, with tree size, and at poor sites. Under future climate scenarios, we forecast increment declines of 22%–117%, while the combined effect of climate and size-related trends results in a 56%–91% decline. Partitioning of forecast uncertainty showed that diameter forecast uncertainty is primarily caused by parameter and initial conditions uncertainty, but increment forecast uncertainty is mostly caused by process error and climate driver uncertainty. This fusion of tree-ring and forest inventory data lays the foundation for robust ecological forecasting of aboveground biomass and carbon accounting at tree, plot, and regional scales, including iterative improvement of model skill.

KEYWORDS

climate change, data fusion, ecological forecasting, forest, forest inventory, ponderosa pine, tree ring

1 | INTRODUCTION

Intergovernmental reports indicate that there are just a few decades left to limit global warming to 1.5°C (IPCC, 2018). Many countries are planning to rely upon nature-based approaches to meet a substantial part of their commitments toward reducing net carbon (C) emissions, and forests are expected to make up ~25% of these emission reductions (Grassi et al., 2017). Specifically, C sequestration by forests has the potential to offset emissions and is one of a few “negative emissions technologies” considered to be affordable and scalable (IPCC, 2018; National Academies of Sciences, 2018), but the response of forests to future climate is highly uncertain (Arora et al., 2020; Bonan, 2008; Friedlingstein et al., 2013; Gatti et al., 2021; Koven et al., 2021; Walker et al., 2020). Elevated atmospheric CO₂, forest recovery from past harvest, and positive responses to warming could all lead to increased carbon sequestration in the future. Negative responses to warming (Babst et al., 2019), increasing tree drought stress (Williams et al., 2020), and tree mortality could reduce forest carbon uptake (Adams et al., 2009; Breshears et al., 2005; Fernández-de-Uña et al., 2016; Lu et al., 2013). Furthermore, interactions between these drivers, including cross-scale interactions, can lead to sudden changes and heterogeneity in future forest carbon dynamics (Becknell et al., 2015; Koontz et al., 2021; Peters et al., 2004; Soranno et al., 2014). Hence, forecasting, managing, and mitigating the response of forest carbon storage and fluxes to climate change is an urgent challenge.

To improve the predictions of complex ecological systems (i.e., model skill), ecologists can adopt techniques that have been used to improve forecasts of other complex systems (e.g., weather forecasting), such as *data fusion* (assimilation), *model validation* with incoming data, and *uncertainty quantification*. *Data fusion* involves combining data streams that are complementary in temporal and or spatial scale (Zipkin et al., 2021). For example, fusing observations of carbon and water fluxes, carbon pools, and vegetation dynamics within an ecosystem model constrains forest carbon cycle predictions for pine plantations across the southeast US (Thomas et al., 2017). In the context of ecological forecasting, *model validation* calls for confronting model predictions with incoming data to evaluate model performance and improve models, known as the “iterative forecasting cycle” (Dietze, 2017). This includes assessing alternative model predictions and which of them best fit the incoming data to evaluate the representation of key ecological processes (Medlyn et al., 2015). *Uncertainty quantification* systematically partitions the drivers of forecast uncertainty, to identify and prioritize actions that can be taken to reduce forecast uncertainty (Clark et al., 2007; Dietze et al., 2018; Fox et al., 2018; Luo et al., 2011). For example, partitioning forecast uncertainty can identify how uncertainties change over time (Dietze, 2017), and whether improving model structure versus honing estimates of parameters would do more to reduce forecast uncertainty (Shiklomanov et al., 2020). Together, these three techniques have driven recent success in constraining carbon cycling and forest productivity predictions (Fer et al., 2018; Fox et al., 2018; Shiklomanov et al.,

2020; Smith et al., 2020; Thomas et al., 2017). Here we take on the problem of forecasting future tree growth using all three of these ingredients of ecological forecasting – *data fusion*, *model validation* with incoming data, and *uncertainty quantification*.

1.1 | Data fusion

To constrain tree growth and the drivers of its variation, we take the approach of fusing tree-ring and forest inventory data, which provide complementary information (DeRose et al., 2017). Tree-rings offer long-term and annually resolved records of the growth of individual trees in response to climate variation, but are usually not available from forest inventory plots, and often lack ecologically relevant meta-data, including information on tree size, local competition, and site characteristics. Forest inventories, such as the US Forest Service Forest Inventory and Analysis (FIA), provide repeated measures of the size of all trees per plot (Bechtold et al., 2005), and hence forest stand density and size structure, along with site-level factors influencing productivity, across an extensive and representative spatial network. Forest inventory measurements are used to quantify decadal trajectories of carbon storage across space (Clark et al., 2007; Domke et al., 2020; Pan et al., 2011), but because revisits to plots are made on a 5- to 10-year basis, they lack the resolution needed to estimate sensitivity to interannual variation in climate. Fusion of these two types of data makes it possible to characterize the many drivers of variation in tree growth (Figure 1): climate, competition, site productivity, and tree size (Babst et al., 2014; Clark et al., 2007; Evans et al., 2017; Schliep et al., 2014). In particular, two-way interactions between these effects may lead to ecological complexity such that tree responses to drought may depend on the intensity of competition, or be contingent on a tree's size (Buechling et al., 2017; Ford et al., 2016; Foster et al., 2016). These ecological contingencies cannot be detected by studying one driver at a time, for example, using traditional methods of sampling and analyzing tree-ring data that focus on climate sensitivity, to the exclusion of other influences on tree growth (i.e., the site and tree selection principles of dendrochronology; Cook, 1990). Leveraging the temporal and spatial strengths of tree-ring data sourced in a forest inventory context with their associated standard forest inventory data (e.g., information on stand-level competition) makes it possible to characterize the complexity of individual tree growth, and offers a promising path to improve predictions of forest carbon cycle dynamics under climate change.

1.2 | Confronting models with data and quantifying uncertainty

Furthermore, we combine model validation with quantification of forecast uncertainty to identify potential model improvements. With revisits to trees scheduled into national forest inventories (USDA Forest Service, 1999), we take advantage of a unique opportunity to *iteratively validate* model predictions with new data

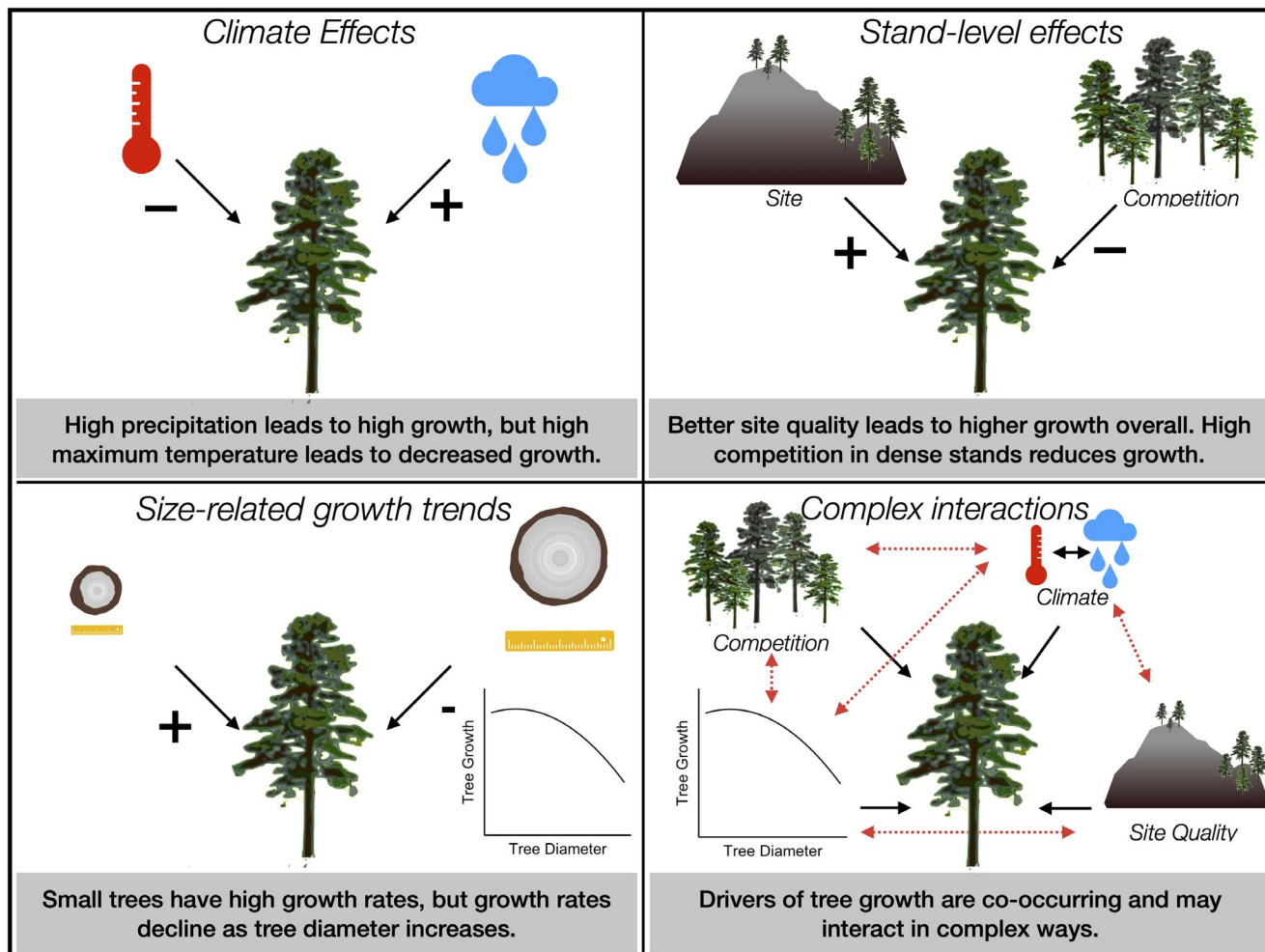










FIGURE 1 Complex ecological interactions driving annual tree growth, carbon uptake, and carbon storage, can lead to uncertainty about the magnitude and direction of response to climate changes. These complex and interacting effects include the impacts of interannual variation in climate, site quality, competitive interactions, size-related growth trends, and interactions between drivers of tree growth

(Dietze et al., 2018) and hence evaluate competing representations of the drivers of variation in tree growth (Babst et al., 2018; DeRose et al., 2017). While model validation identifies and reduces biases in predictions of observed data, analysis of forecast uncertainty can help identify processes or drivers leading to high uncertainty in forecasts of the future. In this way, parsing forecast uncertainty into different components (e.g., initial conditions, driver uncertainty, parameter uncertainty, and additive process error) diagnoses the main drivers of prediction uncertainty and thus highlights different paths to reduce this uncertainty (details in Figure 2).

Here, we use a Bayesian state-space model (Clark et al., 2007) to fuse tree-ring time-series data and spatially extensive FIA plot and tree data (Clark et al., 2007; Evans et al., 2017; Schliep et al., 2014). The development of a tree-ring data network based in the FIA plot network of the interior western US states (DeRose et al., 2017) makes such a fusion of unbiased tree-ring data (compared to traditionally sampled tree-ring

data, i.e., in the ITRDB; Klesse et al., 2018) and other forest inventory data possible. However, assimilation of tree-ring and forest inventory data has not previously been demonstrated at scales larger than a single site. We apply this Bayesian state-space approach to data on *Pinus ponderosa* var. *brachyptera* across the state of Arizona, including >500 trees with increment cores and diameter measurements and >5700 trees with only repeat diameter measurements. This is the first fusion of tree diameter and growth increment on a regional scale. Using the ecological forecasting cycle framework, we then address the following questions: (1) What *ecological complexity* is revealed by explicitly representing multiple drivers of tree growth, along with their cross-scale interactions, for example, the modification of response to climate variability via interaction effects? (2) With ecological complexity explicitly represented, how is tree growth forecasted to change under future climates? (3) What are the main *drivers of uncertainty* in ecological forecasts of tree diameter (C stock) and diameter increment (C flux), and what does uncertainty quantification tell us about avenues for *model improvement*?

Uncertainty Type	Definition	How it is applied here	Increment Uncertainty	Diameter Uncertainty
Initial Conditions	Uncertainty arising from the fact that the true value of initial conditions is not known	95% confidence intervals around DBH estimates at the beginning of our forecasts (year = 2018)		
Parameter	Uncertainty around the true value of parameters in the model	95% confidence intervals around the plot random effects, fixed effects & interactions		
Driver	Uncertainty in the covariate or driver data	Uncertainty in the ensemble of projected future climate drivers		
Process	Uncertainty that is unexplained by the process model, or the residual unexplained variance	Additive process error represented by $\tau_{additive}$		

Using uncertainty partitioning to iteratively improve models

High contribution of **initial condition uncertainty** to total forecast uncertainty can result in highly variable forecasts and may indicate a chaotic system.

High **driver uncertainty** indicates that high uncertainty about the future conditions will lead to high forecast error. Improving estimates of future drivers will reduce driver uncertainty.

Large **parameter uncertainty** can occur when ecological understanding of an effect is highly uncertain. This could be due to divergent responses within a population, low sample size, or stochastic responses. For example, including non-linear and spatially variable responses could reduce parameter uncertainty.

High **process uncertainty** may indicate that some important ecological processes are missing or not accurately represented in model structure. Representation of missing processes through fixed and random effects can reduce process error. Since models are approximations of the truth, process error will never be zero.

FIGURE 2 Types of uncertainty in increment and diameter forecasts, how they are applied in this analysis, and their relative magnitudes in this analysis

2 | METHODS

2.1 | Forest inventory, tree-ring, and climate data

We modeled the size and growth of *Pinus ponderosa* var. *brachyptera* (Engelm.) Lemmon (ponderosa pine) trees across the US southwestern state of Arizona (Figure 3). Forest inventory and tree-ring data were derived from 339 Arizona FIA plots where increment cores had been collected. These plots were

sampled under two different inventory designs: *periodic* inventories before the year 1999, and after 1999, *annual* inventories, in which a temporally and spatially stratified ~10% of plots are sampled each year such that each plot is visited every ~10 years (DeRose et al., 2017; USDA Forest Service, 1999, 2015). Increment cores used in this study were collected from 518 individual trees within the 339 plots during periodic inventories (in 1995 or 1996). Of these trees with increment cores, 260 were in plots carried over to the annual design, whereas 258 were

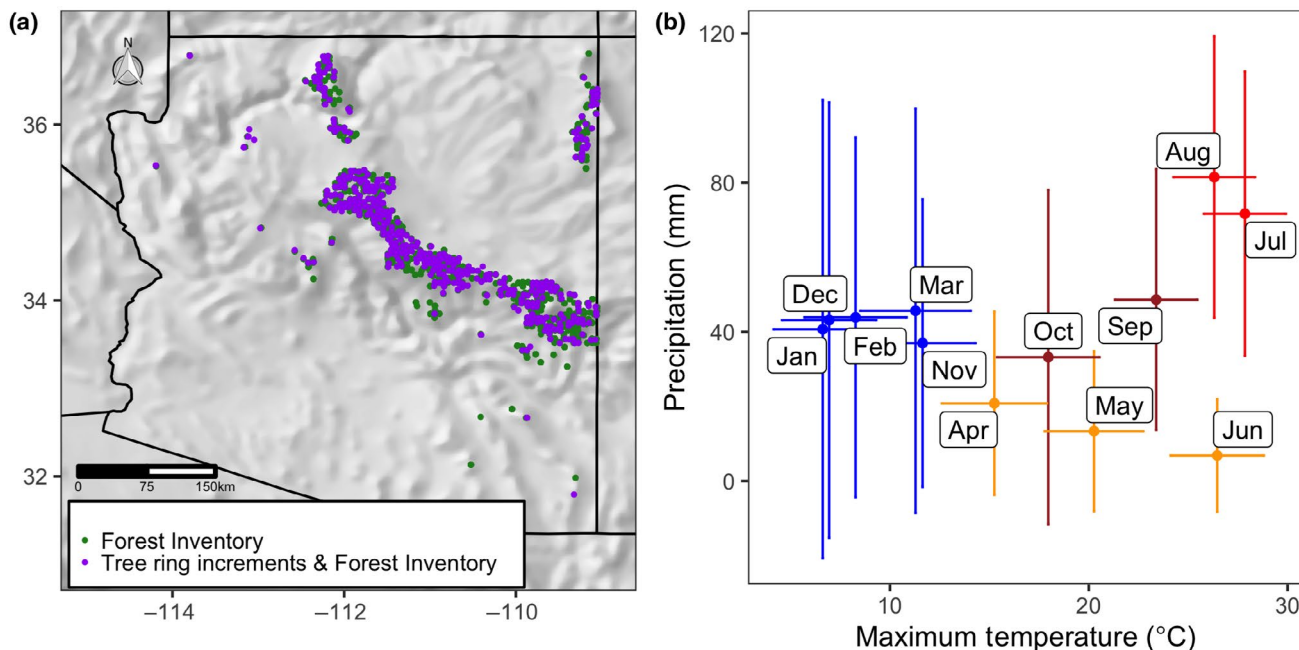


FIGURE 3 (a) Study region and location of *Pinus ponderosa* repeat Forest Inventory measurements and locations of sampled cores. (b) Climatology of sites with *Pinus ponderosa* tree cores. Error bars indicate standard deviation of precipitation and maximum temperature. Colors correspond to four seasons: Blue = winter, yellow = spring + arid foreshummer, red = monsoon, burgundy/dark red = fall

in plots that were “orphaned” after the implementation of the annual design in 1999 – that is, the plot was relocated, and the old plot is no longer monitored. Hence, these 518 trees have 1 or 2 measurements of diameter at breast height (DBH) taken between 1995 and 2010, which we used in model fitting. A subset of these – 186 trees – also have a third DBH measurement taken after 2010, which we held out for use in model validation. Tree-ring records had growth time-series start dates ranging from 1719 to 1978, but because the competitive environment experienced by a tree becomes more uncertain and biased backwards in time from an inventory measurement year (the “fading record” problem; Swetnam et al., 1999), we restricted the tree-ring data used in the analysis to 1965–1996, and estimated diameter from 1965 to 2018. A second pool of tree size and growth data, used in the second stage of model fitting (described below), came from 5794 *P. ponderosa* trees that were located in the same 339 FIA plots and have two DBH measurements between 1995 and 2010, but lack tree-ring data.

Additional forest inventory data used for model fitting were two variables hypothesized to influence tree growth (Figure 1): site index (SI), a plot-level metric of site quality and potential productivity available from the FIA database, and stand density index (SDI), a proxy for the effect of competition. SI is the site-specific expected height of a tree designated as characteristic of the forest type (here, ponderosa pine) at age 50 (Brickell, 1970). We calculated SDI from diameter data on all trees in the subplot and year that the increment core was collected, using the summation method (Shaw, 2000). In reality, SDI is a dynamic variable, because the size and number of trees in a forest change over time. Because

of the challenges associated with reconstructing historical forest stand conditions and past competition (the “fading record” problem, as above), we treated SDI as constant in time, and restricted model fitting to 1965–2018. We also note that absolute SDI potentially confounds site quality, competitive pressure, and disturbance legacy.

We used monthly historical PRISM 4 km resolution climate data products for model fitting over the period from 1965 to 2018 (PRISM Climate Group, Oregon State University, 2004). Correlation analyses between ring width index and a variety of monthly and seasonal mean temperature, maximum temperature, and precipitation variables (see ‘Preliminary Climate correlation analysis’ in Supplemental Materials and Methods S1), along with results from similar analyses reported in the literature (Dannenberg & Wise, 2016; Klesse et al., 2018; McCullough et al., 2017; Williams et al., 2013), led us to include total water-year precipitation and the average of current spring–summer and previous fall maximum temperatures (May–August of the current year and September–October of the previous fall) as predictors of ring-width variability (Supplemental Materials and Methods S1).

2.2 | Bayesian state-space model of tree growth

We fused measurements of growth rings and bole diameter using a Bayesian state-space model, or dynamic linear model, elaborating upon the model introduced by Clark et al. (2007). In this model, bole diameter (DBH), a metric of tree size, is the *state variable* and change

in tree size over time is predicted as a function of the hypothesized drivers illustrated in Figure 1. This model consists of two *data models* (or measurement error models), one of each type of measurement, and a *process model* of the change in DBH from one time step to the next (a difference equation).

2.3 | Data model

In the first data model, DBH measurements $z_{i,t}$ follow a Normal distribution with a mean that is the estimated true diameter of tree i at time t , $x_{i,t}$, and precision τ_{dbh} (where precision is the inverse of variance, $1/\sigma^2$, such that large values of τ indicate low variance). In the second data model, tree-ring measurements are multiplied by 2, converting from radial to diameter increment, and the observed increments $y_{i,t}$ follow a normal distribution truncated at zero, with a mean that is the estimated true diameter increment $inc_{i,t}$, and precision τ_{inc} . We chose the truncation at a very small negative value so the normal distribution can include zero and all positive numbers, consistent with tree-ring data. The true diameter increment, $inc_{i,t}$, is equal to the difference between the true tree diameter at time t and time $t - 1$.

$$inc_{i,t} = x_{i,t} - x_{i,t-1}, \quad (1)$$

$$z_{i,t} \sim \text{normal}(x_{i,t}, \tau_{dbh}), \quad (2)$$

$$y_{i,t} \sim \text{normal}(inc_{i,t}, \tau_{inc}) T(-0.0001). \quad (3)$$

The data models acknowledge the measurement error associated with both data types (i.e., the distinction between observed DBH and true diameter), which makes it possible to reconcile conflicts between them: for example, cumulative growth ring width measurements that are greater or lesser than the difference between sequential DBH measurements. Hence, the “true” diameter of the tree is a latent or unobserved variable, and the two types of observations are used to infer the latent state (size) of the tree through time.

2.4 | Process model

The *process model* describes tree growth as a Markov process with error. The true diameter of each tree i in each year t ($x_{i,t}$) has a mean $DBH_{i,t}$, and additive Normal process error captured by precision τ_{add} . $DBH_{i,t}$ is the sum of the previous year's diameter $x_{i,t-1}$, an intercept μ , a plot-level random intercept modification α_{plot} , a polynomial function of the previous year's diameter (including linear and quadratic terms, $\beta_1 * x_{i,t-1}$ and $\beta_2 * x_{i,t-1}^2$), the effect of SDI, SI, and time-varying climate variables: water-year precipitation and previous-year fall and current-year spring–summer maximum temperatures, as well as all two-way interactions between the fixed effects. All covariates were scaled by the means and standard deviations across space and time, except for the state variable tree size ($x_{i,t-1}$). When used as a covariate, tree size was scaled by subtracting 30 cm from the estimated $x_{i,t-1}$ to improve model convergence and reduce posterior correlations. We explored variations on the process model through model validation (see Section 2.5 below, and Table 1).

$$x_{i,t} \sim \text{normal}(DBH_{i,t}, \tau_{add}), \quad (4)$$

$$\begin{aligned} DBH_{i,t} = & x_{i,t-1} + \mu + \alpha_{plot} + \beta_1 * x_{i,t-1} + \beta_2 * x_{i,t-1}^2 + \beta_3 * SDI + \beta_4 * SI \\ & + \beta_5 * \text{precip} + \beta_6 * T_{max} + \beta_7 * \text{precip} * T_{max} + \beta_8 * SDI \\ & * SI + \beta_9 * SDI * \text{precip} + \beta_{10} * SDI * T_{max} + \beta_{11} * SI \\ & * \text{precip} + \beta_{12} * SI * T_{max} + \beta_{13} * x_{i,t-1} * SI + \beta_{14} * x_{i,t-1} \\ & * SDI + \beta_{15} * x_{i,t-1} * \text{precip} + \beta_{16} * x_{i,t-1} * T_{max}. \end{aligned} \quad (5)$$

Thus, conceptually speaking, the process model follows the linear aggregate model of tree growth described by Cook (1990), which includes covariates accounting for effects operating at different scales, including tree size, stand-scale characteristics, and climate.

Prior distributions assigned to most of the model parameters were weakly informative (Table 1), except for an informative prior assigned to τ_{inc} , the precision associated with tree-ring observations. Initial model fitting revealed strong posterior correlations between

TABLE 1 Priors used in the Bayesian state-space model, their inferred means, 95% CI, and units

Parameter	Prior	Mean	CI	Units
Intercept	$\mu \sim \text{Normal}(0.5, 0.5)$	0.5	-3 to 3	cm
Fixed effects	$\beta \sim \text{Normal}(0, 0.001)$	0	-60 to 60	dimensionless
Plot random intercept	$\alpha_{PLOT} \sim \text{Normal}(0, \tau_{PLOT})$	0	-2 to 2	cm
Diameter observation precision ^a	$\tau_{DBH} \sim \text{Normal}(16, 8)$	2	1-3	precision (1/cm ²)
Additive process precision ^a	$\tau_{add} \sim \text{gamma}(1, 1)$	0.5	0-4	precision (1/cm ²)
Plot random intercept precision ^a	$\tau_{PLOT} \sim \text{gamma}(1, 0.1)$	1	0-0.35	precision (1/cm ²)
Increment observation precision ^a	$\tau_{inc} \sim \text{gamma}(90^2/0.337, 90/0.337)$	90	88-92	precision (1/cm ²)

^aPrecision parameters estimated are the inverse of variance ($\tau = 1/\sigma^2$).

τ_{inc} and the additive process error parameter, τ_{add} , indicating non-identifiability between these two error terms in the model, as described in Dietze (2017, pp. 84–85, 118–119). To address this, we developed an informative prior on τ_{inc} , by asking multiple observers at the University of Arizona Laboratory of Tree Ring Research to measure the same sample of increment cores and modeling those data to estimate τ_{inc} (see additional details in “Informative prior on τ_{inc} ,” Supplemental Materials and Methods S1). We specify the strong informative prior on τ_{inc} , where $a_{\text{inc}}, r_{\text{inc}}$ are determined by the mean and variance of uncertainty around ring widths such that $a_{\text{inc}} = \frac{90^2}{0.337^2}$, and $r_{\text{inc}} = \frac{90}{0.337^2}$.

$$\tau_{\text{inc}} \sim \text{gamma}(a_{\text{inc}}, r_{\text{inc}}). \quad (6)$$

For context, on average, the standard deviation of annual growth measurements across observers is small (0.0097 cm, ranging from 0.0012 to 0.06 cm), and the species-specific prior we assigned to τ_{inc} specifies high precision (mean = 90), translating to a standard deviation similar to that observed among replicated tree-ring measurements ($(1/90)^2 = 0.01$ cm; Table 1).

2.5 | Competing models of tree growth variation

In addition to the full model described above (Equation 5), we also fit a suite of simplified process models that differed with respect to which fixed effects, interaction effects, and random effects were included. Five models yielded satisfactory convergence of posterior parameters: a null model and four candidate models. We describe

these different models of tree growth here and provide their explicit formulation in Table 2.

The “null model” predicts current DBH as a function of the previous year’s DBH plus a size-related trend in ring widths (linear and quadratic terms). Comparing the out-of-sample fit of the null model to the following four alternative models tests whether a more complex process model with additional terms improves the prediction of tree growth (Table 2). The first alternative process model is the “random slope” model (model 2), which includes a plot-level random intercept, a plot-level random modification of the size effect, fixed effects of maximum temperature, precipitation, and competition (SDI), and an interaction between temperature and precipitation, but no interactions between tree size and other fixed effects. The “random slope and interactions” model (model 3) builds on the random slope model by including two-way interactions between tree size, SDI, and the other fixed effects. The “fixed interactions” model (model 4) includes SDI, but not site quality (SI), no plot random effect on the size effect, a plot-level random intercept, and two-way interactions between fixed effects. The “fixed interactions and site quality” model (model 5) has a plot random intercept, no plot random effect on size, and instead includes an additional fixed effect of site quality, along with all the two-way interactions between fixed effects. Model 5 is the process model specified above in Equation (5; Figure 4).

2.6 | Model validation with observed data

We validated our model using out-of-sample measurements of tree diameter from the most recent FIA resurveys of 186 trees in our

TABLE 2 Alternative process model structures and validation statistics

Model number	Model name	Process model	In sample increment		In sample DBH		Validation DBH	
			PPL	RMSPE (cm)	PPL	RMSPE (cm)	PPL	RMSPE (cm)
1	Null model	$DBH_t = X_{t-1} + \beta_X * X_{t-1} + \beta_{X^2} * X_{t-1}^2$	530	0.048	5090	0.703	1244	2.307
2	Random slope	$DBH_t = X_{t-1} + \alpha_{\text{PLOT}} + \beta_{\text{PLOT}(X)} * X_{t-1} + \beta_{X^2} * X_{t-1}^2 + \beta_{\text{SDI}} * \text{SDI} + \beta_{\text{precip}} * \text{Precip} + \beta_{\text{temp}} * T_{\text{max}} + \beta_{\text{precip*temp}} * \text{Precip} * T_{\text{max}}$	264	0.078	4838	0.677	873	1.982
3	Random slope and interactions	$DBH_t = X_{t-1} + \alpha_{\text{PLOT}} + \beta_{\text{PLOT}(X)} * X_{t-1} + \beta_{X^2} * X_{t-1}^2 + \beta_{\text{SDI}} * \text{SDI} + \beta_{\text{precip}} * \text{Precip} + \beta_{\text{temp}} * T_{\text{max}} + \beta_{\text{precip*temp}} * \text{Precip} * T_{\text{max}} + \beta_{\text{precip*SDI}} * \text{Precip} * \text{SDI} + \beta_{\text{temp*SDI}} * T_{\text{max}} * \text{SDI} + \beta_{X*\text{SDI}} * X_{t-1} * \text{SDI} + \beta_{X*\text{precip}} * X_{t-1} * \text{Precip} + \beta_{X*\text{temp}} * X_{t-1} * T_{\text{max}}$	264	0.077	4765	0.694	864	1.969
4	Fixed interactions	$DBH_t = X_{t-1} + \alpha_{\text{PLOT}} + \beta_X * X_{t-1} + \beta_{X^2} * X_{t-1}^2 + \beta_{\text{SDI}} * \text{SDI} + \beta_{\text{precip}} * \text{Precip} + \beta_{\text{temp}} * T_{\text{max}} + \beta_{\text{precip*temp}} * \text{Precip} * T_{\text{max}} + \beta_{\text{precip*SDI}} * \text{Precip} * \text{SDI} + \beta_{\text{temp*SDI}} * T_{\text{max}} * \text{SDI} + \beta_{X*\text{SDI}} * X_{t-1} * \text{SDI} + \beta_{X*\text{precip}} * X_{t-1} * \text{Precip} + \beta_{X*\text{temp}} * X_{t-1} * T_{\text{max}}$	308	0.070	3768	0.603	680	1.783
5	Fixed interactions and site quality	$DBH_t = X_{t-1} + \alpha_{\text{PLOT}} + \beta_X * X_{t-1} + \beta_{X^2} * X_{t-1}^2 + \beta_{\text{SDI}} * \text{SDI} + \beta_{\text{SI}} * \text{SiteIndex} + \beta_{\text{precip}} * \text{Precip} + \beta_{\text{temp}} * T_{\text{max}} + \beta_{\text{precip*temp}} * \text{Precip} * T_{\text{max}} + \beta_{\text{precip*SDI}} * \text{Precip} * \text{SDI} + \beta_{\text{temp*SDI}} * T_{\text{max}} * \text{SDI} + \beta_{X*\text{SDI}} * X_{t-1} * \text{SDI} + \beta_{\text{precip*SI}} * \text{Precip} * \text{SiteIndex} + \beta_{\text{temp*SI}} * T_{\text{max}} * \text{SiteIndex} + \beta_{X*\text{SI}} * X_{t-1} * \text{SiteIndex} + \beta_{X*\text{precip}} * X_{t-1} * \text{Precip} + \beta_{X*\text{temp}} * X_{t-1} * T_{\text{max}}$	307	0.070	4098	0.617	680	1.779

Note: Validation statistics shown are posterior predictive loss (PPL) and root mean squared predictive error (RMSPE).

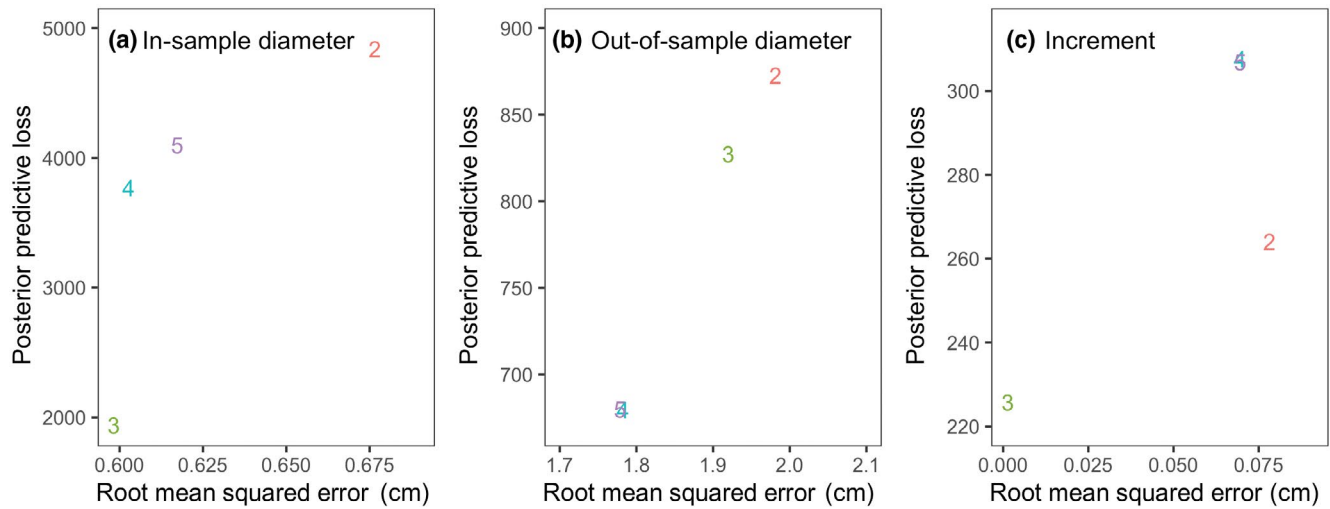


FIGURE 4 Posterior predictive loss and root mean squared prediction error for each model (models 2–5), based on (a) comparison between predicted and observed in-sample diameters, (b) validation between predicted and observed out-of-sample diameters, and (c) comparison between predicted and observed in-sample increment data. Validation statistics are not shown for the Null model, as they were orders of magnitude higher than all other candidate models. Numbers correspond to models in Table 1

dataset. We also evaluated diameter and increment predictions using the DBH and tree-ring increment data that were used in model fitting. We assessed model fit and selected the best-fit model based on root mean-squared predictive error (RMSPE) and posterior predictive loss (PPL). Additionally, we report mean absolute predictive error (MAPE) and validation metrics to assess prediction bias across space and time (V1, V2, V3; Tables S1–S3; Supplemental Materials and Methods S1).

2.7 | Model implementation and convergence

The model was fit using MCMC simulations implemented in JAGS/rjags (Plummer, 2019), using functions from the PEcAn project (<https://pecanproject.github.io/>), on R version 3.6.0 (R Core Team, 2021), Rstudio version 1.2.1335 (Rstudio Team, 2018). These simulations were run on R/Rstudio apps implemented in the Cyverse VICE discovery environment (<https://cyverse.org/>). Each MCMC simulation was run with three chains, an adaptation period of 5000 and 750,000 iterations. Model convergence was evaluated visually using traceplots and Gelman – Rubin diagnostics, which quantify mixing of the posterior parameter chains (Gelman & Rubin, 1992).

During initial model fitting, we attempted to fit a single model using the data from trees without increment cores in addition to trees with increment cores, but these MCMC simulations did not satisfactorily converge because of the large number of poorly constrained latent state variables (e.g., 53 years of annual diameter and increment for the 5794 trees with only 2–3 diameter measurements), with only a small amount of tree-ring data, which are the most information rich data source in terms of informing climate sensitivity (Evans et al., 2017). To address this, we took a two-stage approach to model fitting. We first used the data from the trees with increment cores to estimate model parameters (Stage 1), which converged. We

used the mean and variance of the posterior distributions of parameters from Stage 1 (Table S4) to create a multivariate normal prior on parameters for a second round of model fitting, with inference constrained to the census interval specific to each plot (generally 1994–2010), using only the data from 5794 trees with repeat diameter measurements (Stage 2; see Supplemental Materials and Methods S1). While we had expected Stage 2 to provide additional information on the effects of tree- and stand-level parameters (i.e., tree size, SDI, and SI), parameter estimates are consistent across the two stages. We note that the analyses and figures in this manuscript are based on the stage 1 model, but we present the two-stage approach to demonstrate that it is possible to estimate increment and diameter going back in time for additional trees on the plot, a key step toward future plot-level biomass estimation.

2.8 | Analysis of forecast uncertainty

Future climate projections under four greenhouse gas emissions scenarios, Representative Concentration Pathways (RCP) 2.6, 4.5, 6.0, and 8.5, were used to forecast tree size and growth from 2018 to 2099, based on the final time step of the state variable (tree size) in 2018 ($x_{i,t=2018}$) and posterior estimates of model parameters. These RCPs are scenarios of additional energy retained by the atmosphere, in watts per m^2 , relative to the pre-industrial baseline, as a result of the enhanced greenhouse effect (Taylor et al., 2012). Future climate data were derived from the time-series products of 31 different global climate models (GCMs), downscaled to $\frac{1}{3}$ degree (Reclamation, 2013; Table S5), and bias-corrected at each site using the mean difference (for 1965–2018) between 4 km PRISM historical climate data and each GCM. In these forecast scenarios, SDI and SI are assumed to be constant over time.

To analyze the uncertainty in forecasts of tree diameter and increment, we sequentially added in uncertainty due to five different causes: *initial conditions uncertainty*, the uncertainty surrounding tree size at the start of the forecast time frame; *driver uncertainty*, the uncertainty about future climate conditions (i.e., differences between GCMs); *parameter uncertainty*, the uncertainty surrounding growth model parameters, such as tree growth sensitivity to precipitation or temperature variability; *parameter variability*, caused by unexplained site-to-site heterogeneity (i.e., random effects); and *additive process error*, the variation in tree size and growth not explained by the process model (Figure 2). Initial condition uncertainty was added by sampling from the posterior distribution of the state variable, bole diameter, at the end of our estimated time series (2018), rather than using the posterior mean for each tree. Parameter uncertainty was added by sampling from the joint posterior distribution of all model parameters, rather than using posterior means. To include driver uncertainty, we randomly selected 100 time series of climate variables (water-year precipitation and spring–fall maximum temperature) from the downscaled and bias-corrected GCM projections for each plot. Finally, we included process error by sampling the forecasted tree diameter from a distribution with precision corresponding to the posterior mean estimate of τ_{add} . Sequentially adding in each source of uncertainty, holding the others at their mean, allowed us to partition the contribution of these different sources of uncertainty (Dietze, 2017).

We took a similar first principles approach to parse future driver uncertainty into temperature and precipitation driver components. That is, we sequentially included precipitation and temperature driver uncertainty into future predictions that only included driver uncertainties. Likewise, we parsed parameter-related uncertainty into each fixed effect, random effects, and interaction effects. This allowed us to separate uncertainty surrounding the effects of future climate on tree growth from uncertainty about the value of future climate itself.

3 | RESULTS

3.1 | Assessing model performance

Based on validation with held-out tree diameter measurements, all candidate models reproduced tree diameter better than the null model, with small error and low bias (Figures S10 and S11). Of these alternative models, the “fixed interactions and site quality” model (model 5) best fit our dataset, based on RMSE and PPL for the out-of-sample diameter model validation (Table 1; Tables S1 and S2).

Comparison of predicted diameter increment and observed tree-ring increment demonstrated that the alternative models reproduce tree-ring increments reasonably well, but they systematically underestimate large increments and overestimate small increments (Figures S11 and S12). In contrast to the model validation results for out-of-sample tree diameter, the “random slope and interactions” model (model 3) also had a reasonably good model fit

with respect to RMSE of within-sample increments, as it reduces underestimation of large tree-ring widths (Table S3, Figures S11 and S12).

3.2 | Model effects

Here we report the parameter estimates for the model that best reproduces tree diameter (fixed interactions + site quality, model 5). Estimates for all models are listed in Table S4 and the magnitude and direction of model parameters are qualitatively similar across models 2 through 5. As a reminder, all covariates, apart from our state variable (tree size) were standardized so that slopes of main effects are unitless. SDI had a large negative effect on tree growth in our model ($\beta_{\text{SDI}} = -0.0543$, 95% CI: -0.0675 to -0.0393), and SI had a positive effect on tree growth ($\beta_{\text{SICOND}} = 0.0383$, 95% CI: 0.0240 – 0.0510 ; Figure 5a,b). Fall and spring maximum temperatures had a relatively strong negative effect on tree growth ($\beta_{T_{\text{max}}} = -0.0358$, 95% CI -0.0418 to -0.0298), while water-year precipitation had a positive effect on tree growth ($\beta_{\text{Precipitation}} = 0.0248$, 95% CI: 0.0216 – 0.0281 ; Figure 5c,d). The main and quadratic effects of tree size were both negative ($\beta_X = -0.0036$, 95% CI: -0.0039 to -0.0032 ; $\beta_{X^2} = -0.0001$, 95% CI: -0.0002 to -0.0001), resulting in high growth at low tree diameters, but growth decreases for trees over 25 cm in diameter (Figure 5e, Table S4).

The interaction between water-year precipitation and maximum temperature was slightly positive ($\beta_{\text{Precip} \times T_{\text{max}}} = 0.0037$, 95% CI: 0.0007 – 0.0066), which indicates greater declines in growth in years with dry conditions and high temperatures (Figure 5o). A significant interaction between tree size and temperature ($\beta_{X \times T_{\text{max}}} = -0.0012$, 95% CI: -0.0015 to -0.0008) is such that large diameter trees suffer larger growth declines under high temperatures compared to small trees (Figure 5l). In contrast, a significant interaction between tree size and precipitation ($\beta_{X \times \text{Precip}} = 0.0006$, 95% CI: 0.0003 – 0.0008) results in larger growth declines in small trees under low precipitation (Figure 5k). Finally, there was a significant interaction between SI and maximum temperatures, indicating larger negative effects of high temperature conditions at sites of poor-quality compared to high-quality sites ($\beta_{\text{SI} \times T_{\text{max}}} = 0.0081$, 95% CI: 0.0026 – 0.0140 ; Figure 5f).

Other interaction effects were small in magnitude and had credible intervals overlapping zero, including the interaction between SDI and maximum temperature ($\beta_{\text{SDI} \times T_{\text{max}}} = -0.0053$, 95% CI: -0.0115 to 0.0008 , Figure 5i), and the interaction between precipitation and SDI ($\beta_{\text{SDI} \times \text{Precip}} = -0.0037$, 95% CI: -0.0069 to 0.0004 , Figure 5j), both of which overlap with zero, but are trending negative. Finally, no significant interaction was detected between precipitation and SI ($\beta_{\text{SI} \times \text{Precip}} = -0.0015$, 95% CI: -0.00048 to 0.0017 ; Table S4).

Parameter effects were generally consistent across models, with some minor differences in the magnitude of the effects of diameter (β_X and β_{X^2}) and SDI (Table S4) or interactions involving these effects. The fixed interactions and site quality model (model 5) had a slightly more

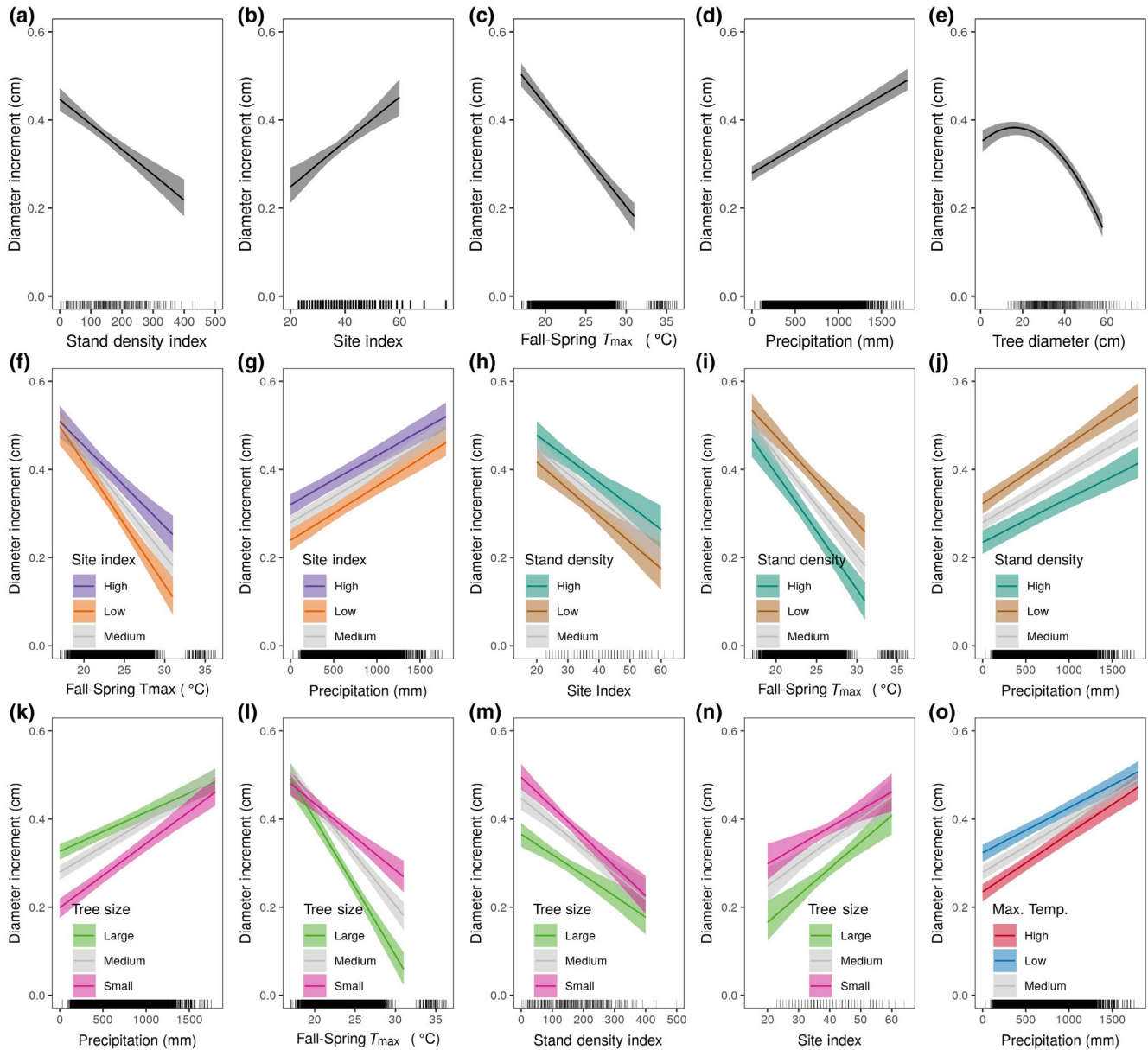


FIGURE 5 Fixed effects and interaction plots conditioned on mean values for all other covariates. Rugs along the x-axis indicate the distribution of data for that covariate. Grey dots indicate the relative magnitude of estimated model parameters. Panels show model effects for each model effect, as follows: (a) stand density index, (b) site index, (c) maximum temperature, (d) water year precipitation, (e) tree size, and interactions between (f) site index and maximum temperature, (g) site index and precipitation, (h) stand density index and site index, (i) stand density index and maximum temperature, (j) stand density index and precipitation, (k) tree size and precipitation, (l) tree size and maximum temperature, (m) tree size and stand density index, (n) tree size and site index, and (o) maximum temperature and precipitation

negative effect of β_{SDI} , compared to models with plot-level random effects on β_X , indicating tradeoffs between plot-level random effects on β_X and fixed effects capturing plot-level differences in quality.

Precision parameters posteriors are reported in Table S1. τ_{inc} has a mean of 89.86 (95% CI: 89.19–90.52), which is equivalent to a standard deviation (SD) around increment observations of about 0.1 cm. The precision parameter on diameter observations, τ_{DBH} , indicates a SD of ~0.78 cm ($\tau_{DBH} = 1.626$, 95% CI: 1.49–1.79). Finally, τ_{add} converted to SD is equivalent to ~0.11 cm ($\tau_{add} = 86.63$, 95% CI: 82.57–90.83).

3.3 | Forecasts

Total uncertainty is greater for forecasts in models with a random effect on tree size, compared to models with only a random intercept and fixed effects. Average total diameter forecast uncertainty for model 3 (random slope and interactions) ranges from 7.5 to 25 cm while total increment forecast uncertainty ranges from 0.9 to 1 cm, when predicted over the timeframe 2018–2099. Forecast uncertainty for model 5 (fixed interactions and site quality) is much lower, ranging from 3.75 to 8.5 cm and 0.62 to 0.65 cm over 2018–2099 for diameter and

increment forecasts, respectively (Figures S9 and S10). For this reason, we focus on forecasts from model 5 in our analysis of uncertainty.

Forecasts from model 5 (fixed interactions and site quality) predict that both changing climate and tree size lead to progressive declines in growth increments across all RCP emissions scenarios. The negative effect of increasing tree size would be expected to drive increment declines of up to ~-40% (range = -66 to -16%) by 2075–2099, even in the absence of climate changes (Figure 6). The direct effects of climate change only (assuming tree size does not change over time) lead to average forecasted growth declines of about -22% (range = -71% to -1%) relative to a scenario of no climate change by 2075–2099, for RCP 2.6 (Figure 6). Under RCPs 4.5, 6.0, and 8.5, growth declines even greater: -51% (-113% to -7%), -55.4% (-156% to -6.6%), and -117% (-207% to -45%), respectively. The two effects together, climate change and increasing tree size, result in a change of -56.9% (range = -104% to -23%), -83.8% (range = -130% to -33.3%), -86.9% (-170% to -31.7%), and -91% (-227% to -15.8%) for RCPs 2.6, 4.5, 6.0, and 8.5, respectively.

Forecasts indicate that many trees experiencing decline will have median growth and/or 95% confidence intervals of growth that drop below zero (Figure S7). This is interpreted as representing the magnitude of stress experienced, which in real trees would translate into growth cessation and an increased risk of mortality (Cailleret et al., 2017; Keane et al., 2001). With greater warming, more trees are forecasted to have median growth that is negative: 6.9% of trees, 10.4% of trees, 25.1% of trees, and 52.1% of trees for RCPs 2.6, 4.5, 6.0, and 8.5, respectively.

3.4 | Partitioning forecast uncertainty

Partitioning forecast uncertainty implicates different drivers of forecast uncertainty for increments versus tree diameter. Process uncertainty is the largest driver of increment uncertainty, comprising >60% of the total increment uncertainty across all time periods and RCP scenarios. Driver uncertainty is the second largest contributor to increment uncertainty, and increases from ~20% of total uncertainty from 2020 to 2049 to >25% of total uncertainty after 2075, and increases under higher emissions scenarios. Parameter uncertainty comprises almost 1%–2% of the increment uncertainty across the forecast period. Random effect uncertainty makes up >3% of the increment uncertainty in 2020–2049, but decreases to <3% over time. Initial condition uncertainty makes up <0.5% of the increment uncertainty.

For tree diameter, initial condition uncertainty makes up (on average) ~55% of the total uncertainty between 2020 and 2049, but declines rapidly over time to <5% after 2075. In contrast, the contribution of parameter uncertainty is initially ~6%, but increases to >15% by 2075–2099. The contribution of random effect uncertainty also increases over time, from almost 20% between 2020 and 2049, to >35% after 2050. There is little variation in the contribution of each component to forecast uncertainty across the different RCP scenarios for diameter (Figure 7c,f). Driver uncertainty initially

contributes very little to diameter uncertainty, making up <10% of uncertainty from 2020 to 2049, but increases to >25% after 2050. Finally, process uncertainty also is a small fraction of diameter forecast uncertainty, making up ~8%–14% of total uncertainty across time periods.

Precipitation and temperature each contributed substantially to driver uncertainty. For forecasts of growth increment, on average 35% (range = 7.4%–69%) of the driver uncertainty was attributable to precipitation uncertainty and ~65% to temperature uncertainty (range = 31%–92.6%; Figure 8a). For forecasts of tree diameter, about 18% of the driver uncertainty is due to uncertainty about projected future precipitation and 82% to uncertainty about future temperature (Figure 8b). The contribution of temperature uncertainty increases both over time and with RCP scenarios, with strong interannual variability.

The contribution of each fixed effect to total parameter uncertainty followed the same ranking for both diameter and increment forecasts (Figure 8c,d). Uncertainty about the effect of tree size contributed the most to parameter uncertainty (~25%). The second largest causes of parameter uncertainty are related to stand-level effects, SI and SDI, which each make up 15%–20% of total parameter uncertainty. The third largest source of uncertainty is due to the sensitivity of diameter and increment to variation in maximum temperature (~14%), and interactions involving temperature sensitivity contribute additional temperature-related uncertainty to our forecasts, including the interactions between temperature and tree size (6%), temperature and SDI (5%), and temperature and precipitation (1%). In contrast, uncertainty about precipitation sensitivity is low – contributing just 1%. Interactions between site index and tree size contribute ~4%. All other interactions each contribute less than 1% of the total parameter uncertainty.

4 | DISCUSSION

Applying principles of ecological forecasting, we characterized the complexity of tree growth, evaluated alternative models of the growth process, forecast future tree size and growth, and used forecast uncertainty quantification to identify avenues for improving skill at forecasting future forest carbon stocks and fluxes. The first of these principles of ecological forecasting was to fuse two complementary data sources, tree-ring and forest inventory data, to parse multiple and interacting drivers of tree growth in a way that would be difficult to achieve with either data source alone. In particular, we found that tree- and stand-level factors, such as tree size, site quality, and competition, modify climate responses in a manner that could generate landscape-scale heterogeneity in climate vulnerability, and be leveraged toward management of forest resilience to climate stress. We then used model assessment and validation to judge alternative process models of tree growth, revealing tradeoffs between different targets of model optimization. Forecasts using a parsimonious model that best predicted out-of-sample diameter data showed, on average, a 56%–91%

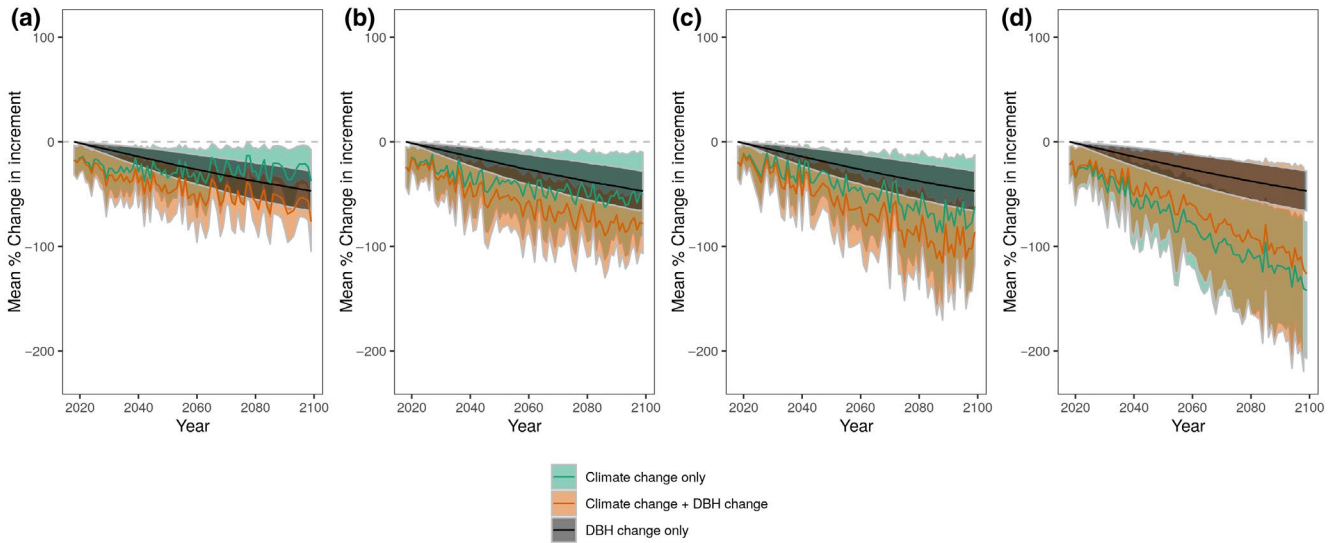


FIGURE 6 Median percent change in diameter increment under conditional forecasts due to climate changes only, DBH changes only, and change in both climate and tree size. Percent change relative to forecasts made with no change in climate and no change in tree size. Forecasts shown for (a) RCP 2.6, (b) RCP 4.5, (c) RCP 6.0, and (d) RCP 8.5. Lines are median % change, shading represents 95% quantiles across all 518 tree-level forecasts

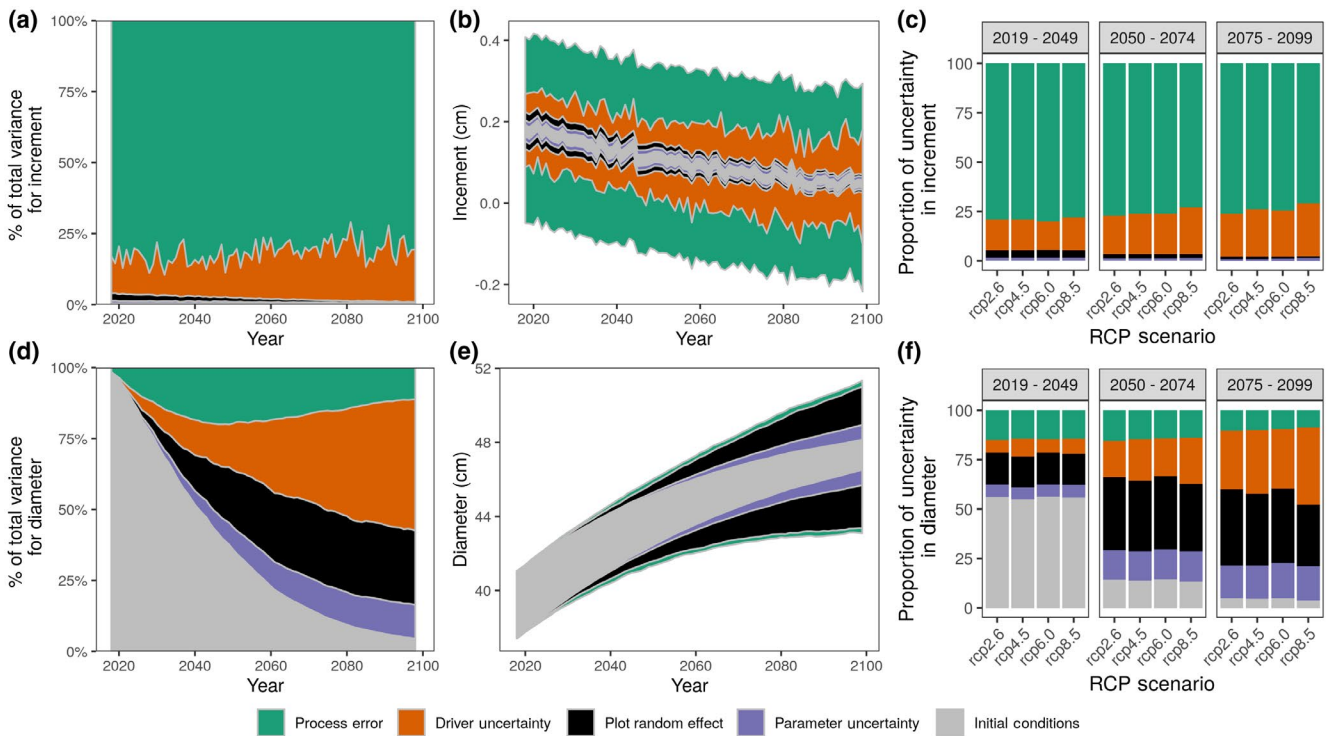


FIGURE 7 Forecasts and partitioning of forecast uncertainty for diameter increment (top) and tree diameter (bottom) under future climate projections. (a) Proportion of uncertainty for increment forecasts of a single tree under RCP 8.5. (b) Forecast of increment for the same single tree with uncertainty partitioning. (c) Proportion of uncertainty that contributes to increment forecasts, averaged across all 518 trees. (d) Proportion of uncertainty for Diameter forecasts of a single tree. (e) Forecasts of the same single tree diameter with uncertainty partitioning. (f) Proportion of uncertainty contributing to uncertainty in diameter forecasts, averaged across all 518 trees

decline in tree diameter increment across RCP scenarios, underscoring how critical emissions reductions are to preserving forest carbon sequestration. Finally, a systematic analysis of forecast uncertainty revealed contrasting drivers of uncertainty in diameter

(carbon stocks) vs. diameter increment (carbon fluxes), with divergent avenues for improvement of forecasts. In the following, we highlight insights gained from each of these steps in the ecological forecasting cycle.

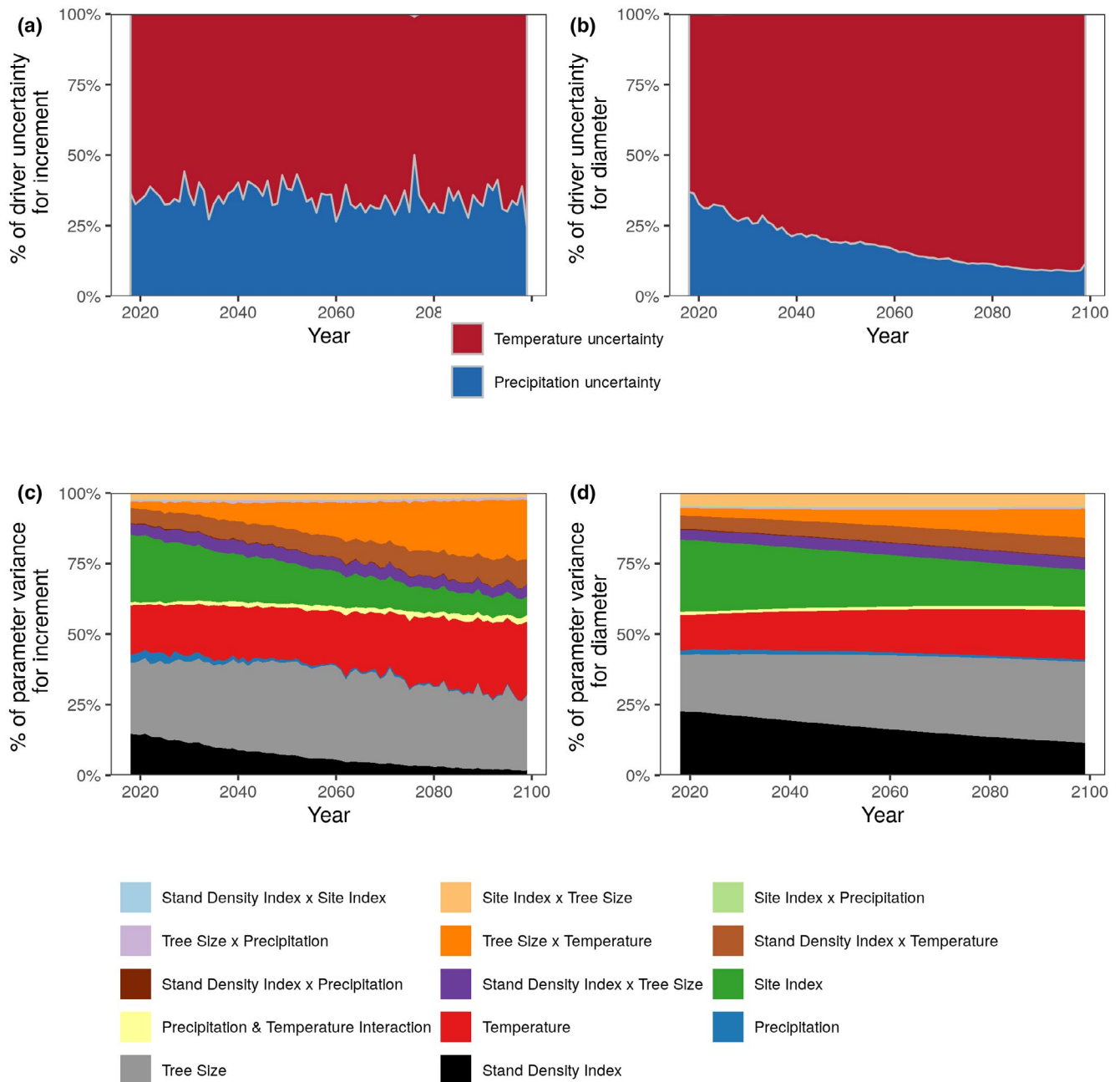


FIGURE 8 Proportion of uncertainty due to different drivers (a, b) and different parameters (c, d). Uncertainty partitioning is shown for both increment (a, c) and tree diameter (b, d), as the average proportion of uncertainty across all trees and RCP scenarios

4.1 | Tree growth is a complex ecological process

Tree-ring and forest inventory data each bring their own strengths to the problem of modeling tree growth, namely the annual resolution necessary to detect climate sensitivity, and information on tree- and site-level drivers. By fusing the two together, we were able to model tree growth as a function of multiple drivers acting simultaneously, including interactions between them. Plot-level factors have the greatest impact on bole diameter increments: growth increments increase with site index (SI) and decline with stand density index (SDI); Buechling et al., 2017; Ford et al., 2016; Kunstler et al., 2010; McLeod

& Running, 2011; Zhang et al., 2011, 2019). These two factors should generate spatial heterogeneity in growth rates and C stock. At the tree scale, growth increments are larger when bole diameter is small and decline as bole diameter increases, reflecting a geometric effect of tree size on growth (Bowman et al., 2013). Model-estimated climate effects all point to sensitivity of *P. ponderosa* var. *brachyptera* growth and C uptake to drought. Maximum temperatures negatively affect tree growth, and water-year precipitation positively affects tree growth (McCullough et al., 2017; Peltier & Ogle, 2019). Thus, tree growth is indeed a complex ecological process, influenced by several factors simultaneously, operating at scales from tree to

stand to landscape: tree size, biophysical setting, competition, and climate. Resolving uncertainties about forest carbon dynamics requires that all these drivers be considered together.

4.2 | Cross-scale interactions modify climate responses

Adding to this complexity are interactions between drivers of tree growth. For example, the effects of temperature and precipitation interact such that a year of low precipitation leads to even lower growth if temperatures are high, supporting the idea that high atmospheric demand for moisture (high vapor pressure deficit) is a particularly potent form of drought stress (Breshears et al., 2005; McDowell et al., 2016; Williams et al., 2013, 2020). Tree-level factors then modify these climate sensitivities: small trees suffered a greater reduction in growth than large trees in the face of a lack of precipitation, whereas the opposite was true under hot conditions (Figure 5k,l). While large diameter trees are not always the tallest, our findings are consistent with previous work on interactions between tree size and climate with *P. ponderosa* which show that canopy-dominant trees are more sensitive to temperature fluctuations, whereas intermediate canopy trees are more sensitive to precipitation (Carnwath et al., 2012). Because they must lift water higher, tall trees experience high hydraulic pressure (Darcy's Law) and thus high cavitation risk under elevated temperatures, growth declines, and even mortality during the warm droughts that can be expected in the future (Adams et al., 2009; Breshears et al., 2005; Koch et al., 2004; McDowell & Allen, 2015; Stovall et al., 2019; Williams et al., 2013, 2020). However, these same mature trees may be more resilient to precipitation-driven droughts, perhaps due to extensive rooting structures accessing deeper soil moisture or greater soil volume (Domec et al., 2004). Thus, hotter future droughts may put tall, canopy dominant, high biomass trees at risk, leading to stand-level losses in C storage, whereas droughts driven primarily by low precipitation may put small trees at greater risk, potentially limiting recruitment and regeneration of forest stands.

Cross-scale interactions between site quality, competition, and climate sensitivity can drive heterogeneity in climate responses, which highlights potential management interventions that could promote climate resilience. Based on our analysis, *Pinus ponderosa* var. *brachyptera* trees at higher-quality sites fare better under climate extremes, pointing to heterogeneity in vulnerability to climate stress that could be taken advantage of in landscape-scale management aimed at increasing forest resilience to climate change. Interactions between site-level competition and climate indicate that dense stands of ponderosa pine are more susceptible to the negative effects of high temperature and low precipitation over the time period of our study, consistent with previous work (Buechling et al., 2017; Ford et al., 2016; Foster et al., 2016; Kunstler et al., 2010; Zhang et al., 2011). These interactions involving competition suggest that thinning and prescribed fire are management tools that could increase tree-level resilience to climate stress, enhance tree-level

carbon uptake, and reduce mortality risk in these forests (Campbell et al., 2009; Sohn et al., 2016; Zhang et al., 2019). Since we explicitly quantify how stand-level processes modulate tree-level climate response through interaction effects and their uncertainties, our approach could be used to identify forest stands that would benefit most from management interventions and the levels of density reduction, achieved via thinning, that would be needed to offset the negative impacts associated with climate change.

4.3 | Confronting model predictions with data reveals tradeoffs

Confronting predictions made by alternative models with data in two ways, through model assessment (evaluation of competing model predictions using calibration data) and model validation via the "ecological forecasting cycle" (evaluation of competing model predictions using newly collected, incoming data), we identified tradeoffs between different targets of model optimization. While all candidate models were biased toward underestimating large increments and overestimating small increments, the inclusion of plot-level modification (random effects) of the effect of tree size (e.g., model 3) reduced these biases, by capturing heterogeneity in this effect. However, forecasts from model 3 have about twice as much uncertainty in diameters and increments (Figures S9 and S10) because the large number of random effects increases model complexity. In other words, we found a tradeoff between model fit to calibration data and forecast uncertainty. Model validation with out-of-sample diameter data, that is, from scheduled forest inventory remeasurements, highlighted a second tradeoff, between model performance with respect to predicting tree diameter vs. diameter increment. Adding more random effects improved increment prediction (i.e., model 3, the random effects and interactions model), but the model with more fixed effects (i.e., model 4, the fixed effects model and model 5, the fixed effects and site quality model) improved diameter prediction. Thus, we used model 5 (the fixed interactions and site quality model) to forecast and partition forecast uncertainty, because it is both a more parsimonious process model (less random effects) and it performed best with respect to out-of-sample validation of tree diameter.

4.4 | Forecasts indicate widespread future growth declines

Given the strong negative sensitivity of *P. ponderosa* growth to temperature, and projected future climate that is much warmer than the 1965–2000 baseline (IPCC, 2014; Williams et al., 2013, 2020), climate change alone is projected to drive a 22%–117% (RCP 2.6–RCP 8.5) average decline in diameter increment by 2099, with relatively high uncertainty indicating that up to 51%–227% growth declines are possible (upper 95% quantiles for RCP 2.6–RCP 8.5). Diameter increments will also decline as trees (inevitably) get larger over time. Size-related trends alone would lead to a ~40% decline in diameter

increments. However, since climate-stressed trees grow more slowly, leading to smaller annual increases in tree size and a weaker size-related decline in growth increments, including both drivers of change in growth lead to an additional ~20%–36% decline in diameter increment, compared to just climate-driven change. Though there is substantial uncertainty surrounding these forecasts, the trends are clear: significant growth declines are expected, which increase with the strength of the enhanced greenhouse effect (RCPs). It is important to point out that these forecasts are conditioned on the current distributions of tree size, competition, and site quality in our dataset, which will in fact change in the future. Furthermore, they are forecasts of diameter increment, rather than volume-based metrics (basal area or biomass increments); they are not forecasts of change in annual carbon sequestration at the whole-tree or forest stand scales.

Nonetheless, it is clear that without targeted management to mitigate climate stress, we should expect the negative effects of warming to slow the rate of tree-level carbon uptake and reduce carbon storage. Indeed, under RCP 8.5, median forecasted growth increments fall below zero for >52% of trees during the projection time period. This is congruent with other studies, using physiological data and dynamic vegetation models, which have predicted >50% tree mortality in ponderosa pine forests (McDowell et al., 2016), and large-scale forest die-off under a warmer future (Adams et al., 2009; Breshears et al., 2005; McDowell & Allen, 2015; Williams et al., 2013). While we do not model mortality explicitly here, consistently declining growth rates and average modeled growth rates below zero suggest that these trees would be at increased risk of mortality (Cailleret et al., 2019).

4.5 | Uncertainty quantification identifies multiple avenues for model improvement

Uncertainty partitioning revealed key differences between forecasting of carbon pool versus flux (i.e., tree size vs. growth), suggesting different paths for model improvement. Diameter forecast uncertainty accumulates over time, and is primarily driven by parameter uncertainty (fixed and random effects). In contrast, increment forecast uncertainty is stable over time (see also Alexander et al., 2018), and is primarily caused by process and driver uncertainty. The strong contribution of parameter uncertainty to relatively high uncertainty about carbon storage (tree diameter) over time indicates that effects could be better characterized with more data or more accurately portrayed in the process model (Shiklomanov et al., 2020). For example, uncertainty about the effect of competition (SDI) could be reduced by incorporating additional FIA data to estimate SDI as a time-varying predictor of growth. Substantial uncertainty surrounding the effect of temperature suggests that adding more tree-ring data from a wider range of mean temperatures, modeling spatial variation in temperature sensitivity (Canham et al., 2018; Fritts et al., 1965; Klesse et al., 2018; McCullough et al., 2017), and fitting the data to physiologically based nonlinear temperature

responses (McDowell & Allen, 2015; McDowell et al., 2016; Stout & Sala, 2003) could all reduce forecast uncertainty. In contrast, if we work with just the data in hand, the large contribution of parameter uncertainty at longer timescales implies that we may want to consider using simpler models with fewer parameters for longer-term predictions. Indeed, the models without plot-level modifiers on the effect of tree size (models 4 and 5) have much lower total forecast uncertainty (Figures S8 and S9). This pattern of model selection favoring reduced model complexity with lead time is consistent with both first principles (Dietze, 2017) and other ecological forecasts (Carey et al., 2021).

The strong contribution of process and random effect uncertainty to forecasts of growth increment highlights a need both for more data and for explicit consideration of ecological processes expected to cause site-to-site heterogeneity in tree growth. This includes fire and insect disturbances, which can create spatial heterogeneity in stand structure and climate sensitivity (Allen et al., 2002; Brown & Wu, 2005; Ehle & Baker, 2003; Itter et al., 2017; Lundquist & Negron, 2000; Parker et al., 2006; Zhang et al., 2019), drought legacy effects that may vary over time or space (Ogle et al., 2015; Peltier & Ogle, 2019), and spatial differences in soil quality and site characteristics that impact potential productivity (Carnwath et al., 2012; McLeod & Running, 2011; Zhang et al., 2011). Since plot-level random slopes on the effect of tree size reduced increment prediction bias in model assessments, a more explicit representation of how allometry varies with site-level factors is another avenue for improving forecasts of C flux (Bond et al., 2007; Bowman et al., 2013). The fact that process error makes up a greater proportion of the uncertainty about future increment compared to future diameter may reflect the influence of these “missing” forest processes, which largely affect short-term responses, but are averaged out over longer timescales. Alternatively, this difference may reflect a need to account for temporal autocorrelation in the process error. Furthermore, given that diameter forecasts are dominated by parameter error, and that we found a tradeoff between model fit to calibration data and forecast uncertainty (see Section 4.3), adding complexity to the process model to improve prediction of interannual growth variability may, counterintuitively, increase the uncertainty in long-term diameter and carbon sequestration forecasts.

Finally, sub-partitioning the uncertainty caused by future temperature versus precipitation lends insight into how the climate-related component of forecast uncertainty could be reduced. Precipitation contributes to a third or over half of the driver uncertainty for some trees, reflecting high interannual and inter-model variability in projections of future precipitation, despite only small forecasted changes in average precipitation. However, there is high confidence about the effect of precipitation on tree growth (low parameter uncertainty), leading to lower overall precipitation-related uncertainty. In contrast, the ensemble of CMIP5 climate model projections all project that temperature will increase in the future (IPCC, 2014; Williams et al., 2013, 2020), leading to an increase in the contribution of temperature to driver uncertainty for diameter forecasts over time, and there is relatively high uncertainty about

the effect of temperature on tree growth. Furthermore, ecological contingencies involving temperature, that is, cross-scale interactions between temperature and tree size, and temperature and site factors (SDI, SI), also contribute considerably to parameter uncertainty, underscoring how critical it is to nail down these interactions to reduce uncertainty surrounding the response of forest carbon uptake and storage to rising temperatures and to accomplish robust C accounting.

4.6 | Toward carbon accounting with tree-ring and forest inventory data

Our study adds to a growing body of literature linking tree-ring data and forest inventories to constrain the carbon cycle and model carbon dynamics (Biondi, 1999; Dye et al., 2016; Graumlich et al., 1989; Lara et al., 2013; Schliep et al., 2014). Bayesian data fusion of tree-ring data and diameter data within a state-space model has previously been implemented at local, single site scales (Clark et al., 2007; Schliep et al., 2014). Here, we demonstrate that this approach can be used to forecast diameter and growth of trees at a multi-site, regional scale. Furthermore, fusing climate-sensitive tree-ring data with additional tree and plot-level information from forest inventory data shows that complex and interacting drivers of tree growth can result in heterogeneity in forest carbon uptake and storage, underscoring the need to move beyond mean-field forecasts of tree growth. While national forest inventories, such as the USFS FIA program, are already used to measure, verify, and predict forest C uptake and storage (Domke et al., 2020; Zald et al., 2016), fusing inventory data and tree-ring data is an indispensable tool to characterize the ecological complexity (i.e., cross-scale interactions) driving forest growth, and thus resolve uncertainties about the effect of climate change on forest carbon dynamics. In this context, our analysis lays the foundation to develop a national system of ongoing forest carbon accounting and iterative carbon cycle forecasts that are constrained by tree-ring data and annual forest inventories. Large-scale carbon accounting and analysis of carbon cycle uncertainties provide a predictive framework to assess potential for using forests as negative emissions technologies for atmospheric CO₂ drawdown, critical for mitigating the most drastic negative effects of global climate change.

ACKNOWLEDGMENTS

We thank Tyson Swetnam for his assistance with developing R/ rstudio apps to run our Bayesian analysis, which was made possible through CyVerse's External Collaborative Partnership program. This material is based upon work conducted using CyVerse, which is supported by the National Science Foundation under Award Numbers DBI-0735191, DBI-1265383, and DBI-1743442. URL: www.cyverse.org. MCD was supported by NSF 1458021, 1638577, and 1702996. KAH and MEKE were supported by NSF MSB 1802893.

CONFLICT OF INTEREST

The authors declare no conflict of interest.

DATA AVAILABILITY STATEMENT

The data that support the findings of this study are openly available through Cyverse Data Commons and can be accessed through <https://doi.org/10.25739/sd83-rk24>.

ORCID

Kelly A. Heilman  <https://orcid.org/0000-0001-5932-1317>

Michael C. Dietze  <https://orcid.org/0000-0002-2324-2518>

Alexis A. Arizpe  <https://orcid.org/0000-0001-8127-3999>

John D. Shaw  <https://orcid.org/0000-0002-5797-1006>

Andrew O. Finley  <https://orcid.org/0000-0002-2277-2912>

Stefan Klesse  <https://orcid.org/0000-0003-1569-1724>

R. Justin DeRose  <https://orcid.org/0000-0002-4849-7744>

Margaret E. K. Evans  <https://orcid.org/0000-0003-3220-3382>

REFERENCES

- Adams, H. D., Guardiola-Claramonte, M., Barron-Gafford, G. A., Villegas, J. C., Breshears, D. D., Zou, C. B., Troch, P. A., Huxman, T. E., & Mooney, H. A. (2009). Temperature sensitivity of drought-induced tree mortality portends increased regional die-off under global-change-type drought. *Proceedings of the National Academy of Sciences of the United States of America*, *106*, 7063–7066. <https://doi.org/10.1073/pnas.0901438106>
- Alexander, M. R., Rollinson, C. R., Babst, F., Trouet, V., & Moore, D. J. P. (2018). Relative influences of multiple sources of uncertainty on cumulative and incremental tree-ring-derived aboveground biomass estimates. *Trees*, *32*, 265–276. <https://doi.org/10.1007/s00468-017-1629-0>
- Allen, C. D., Savage, M., Falk, D. A., Suckling, K. F., Swetnam, T. W., Schulke, T., Stacey, P. B., Morgan, P., Hoffman, M., & Klingel, J. T. (2002). Ecological restoration of southwestern ponderosa pine ecosystems: A broad perspective. *Ecological Applications*, *12*, 1418–1433. <https://doi.org/10.2307/3099981>
- Arora, V. K., Katavouta, A., Williams, R. G., Jones, C. D., Brovkin, V., Friedlingstein, P., Schwinger, J., Bopp, L., Boucher, O., Cadule, P., Chamberlain, M. A., Christian, J. R., Delire, C., Fisher, R. A., Hajima, T., Ilyina, T., Joetzer, E., Kawamiya, M., Koven, C. D., ... Ziehn, T. (2020). Carbon-concentration and carbon-climate feedbacks in CMIP6 models and their comparison to CMIP5 models. *Biogeosciences*, *17*, 4173–4222. <https://doi.org/10.5194/bg-17-4173-2020>
- Babst, F., Bodesheim, P., Charney, N., Friend, A. D., Girardin, M. P., Klesse, S., Moore, D. J. P., Seftigen, K., Björklund, J., Bouriaud, O., Dawson, A., DeRose, R. J., Dietze, M. C., Eckes, A. H., Enquist, B., Frank, D. C., Mahecha, M. D., Poulter, B., Record, S., ... Evans, M. E. K. (2018). When tree rings go global: Challenges and opportunities for retro- and prospective insight. *Quaternary Science Reviews*, *197*, 1–20. <https://doi.org/10.1016/j.quascirev.2018.07.009>
- Babst, F., Bouriaud, O., Alexander, R., Trouet, V., & Frank, D. (2014). Toward consistent measurements of carbon accumulation: A multi-site assessment of biomass and basal area increment across Europe. *Dendrochronologia*, *32*, 153–161. <https://doi.org/10.1016/j.dendro.2014.01.002>
- Babst, F., Bouriaud, O., Poulter, B., Trouet, V., Girardin, M. P., & Frank, D. C. (2019). Twentieth century redistribution in climatic drivers of global tree growth. *Science Advances*, *5*, eaat4313. <https://doi.org/10.1126/sciadv.aat4313>
- Bechtold, W. A., & Patterson, P. L. (Eds.). (2005). *The enhanced forest inventory and analysis program—National sampling design and estimation procedures*. Gen Tech Rep SRS-80. US Department of Agriculture Forest Service Southern Research Station. 85 P 080. <https://doi.org/10.2737/SRS-GTR-80>

- Becknell, J. M., Desai, A. R., Dietze, M. C., Schultz, C. A., Starr, G., Duffy, P. A., Franklin, J. F., Pourmokhtarian, A., Hall, J., Stoy, P. C., Binford, M. W., Boring, L. R., & Staudhammar, C. L. (2015). Assessing interactions among changing climate, management, and disturbance in forests: A macrosystems approach. *BioScience*, *65*, 263–274. <https://doi.org/10.1093/biosci/biu234>
- Biondi, F. (1999). Comparing Tree-ring chronologies and repeated timber inventories as forest monitoring tools. *Ecological Applications*, *9*, 216–227.
- Bonan, G. B. (2008). Forests and climate change: Forcings, feedbacks, and the climate benefits of forests. *Science*, *320*, 1444–1449. <https://doi.org/10.1126/science.1155121>
- Bond, B. J., Czarnomski, N. M., Cooper, C., Day, M. E., & Greenwood, M. S. (2007). Developmental decline in height growth in Douglas-fir. *Tree Physiology*, *27*, 441–453. <https://doi.org/10.1093/treephys/27.3.441>
- Bowman, D. M. J. S., Brienen, R. J. W., Gloor, E., Phillips, O. L., & Prior, L. D. (2013). Detecting trends in tree growth: Not so simple. *Trends in Plant Science*, *18*, 11–17. <https://doi.org/10.1016/j.tplants.2012.08.005>
- Breshears, D. D., Cobb, N. S., Rich, P. M., Price, K. P., Allen, C. D., Balice, R. G., Romme, W. H., Kastens, J. H., Floyd, M. L., Belnap, J., Anderson, J. J., Myers, O. B., & Meyer, C. W. (2005). Regional vegetation die-off in response to global-change-type drought. *Proceedings of the National Academy of Sciences of the United States of America*, *102*, 15144–15148. <https://doi.org/10.1073/pnas.0505734102>
- Brickell, J. E. (1970). *Equations and computer subroutines for estimating site quality of eight Rocky Mountain species*. (No. INT-75), Res. Pap. U.S. Department of Agriculture, Forest Service.
- Brown, P. M., & Wu, R. (2005). Climate and disturbance forcing of episodic tree recruitment in a southwestern ponderosa pine landscape. *Ecology*, *86*, 3030–3038. <https://doi.org/10.1890/05-0034>
- Buechling, A., Martin, P. H., & Canham, C. D. (2017). Climate and competition effects on tree growth in Rocky Mountain forests. *Journal of Ecology*, *105*, 1636–1647. <https://doi.org/10.1111/1365-2745.12782>
- Cailleret, M., Dakos, V., Jansen, S., Robert, E. M. R., Aakala, T., Amoroso, M. M., Antos, J. A., Bigler, C., Bugmann, H., Caccianaga, M., Camarero, J.-J., Cherubini, P., Coyea, M. R., Čufar, K., Das, A. J., Davi, H., Gea-Izquierdo, G., Gillner, S., Haavik, L. J., ... Martínez-Vilalta, J. (2019). Early-warning signals of individual tree mortality based on annual radial growth. *Frontiers in Plant Science*, *9*. <https://doi.org/10.3389/fpls.2018.01964>
- Cailleret, M., Jansen, S., Robert, E. M. R., Desoto, L., Aakala, T., Antos, J. A., Beikircher, B., Bigler, C., Bugmann, H., Caccianiga, M., Čada, V., Camarero, J. J., Cherubini, P., Cochard, H., Coyea, M. R., Čufar, K., Das, A. J., Davi, H., Delzon, S., ... Martínez-Vilalta, J. (2017). A synthesis of radial growth patterns preceding tree mortality. *Global Change Biology*, *23*, 1675–1690. <https://doi.org/10.1111/gcb.13535>
- Campbell, J., Alberti, G., Martin, J., & Law, B. E. (2009). Carbon dynamics of a ponderosa pine plantation following a thinning treatment in the northern Sierra Nevada. *Forest Ecology and Management*, *257*, 453–463. <https://doi.org/10.1016/j.foreco.2008.09.021>
- Canham, C. D., Murphy, L., Riemann, R., McCullough, R., & Burrill, E. (2018). Local differentiation in tree growth responses to climate. *Ecosphere*, *9*, e02368. <https://doi.org/10.1002/ecs2.2368>
- Carey, C. C., Woelmer, W. M., Lofton, M. E., Figueiredo, R. J., Bookout, B. J., Corrigan, R. S., Daneshmand, V., Hounshell, A. G., Howard, D. W., Lewis, A. S. L., McClure, R. P., Wander, H. L., Ward, N. K., & Thomas, R. Q. (2021). Advancing lake and reservoir water quality management with near-term, iterative ecological forecasting. *Inland Waters*, *1*–14. <https://doi.org/10.1080/20442041.2020.1816421>
- Carnwath, G. C., Peterson, D. W., & Nelson, C. R. (2012). Effect of crown class and habitat type on climate–growth relationships of ponderosa pine and Douglas-fir. *Forest Ecology and Management*, *285*, 44–52. <https://doi.org/10.1016/j.foreco.2012.07.037>
- Clark, J. S., Wolosin, M., Dietze, M., Ibáñez, I., LaDeau, S., Welsh, M., & Kloeppel, B. (2007). Tree growth inference and prediction from diameter censuses and ring widths. *Ecological Applications*, *17*, 1942–1953. <https://doi.org/10.1890/06-1039.1>
- Cook, E. (1990). *Methods of dendrochronology—Applications in the environmental sciences*. Kluwer Academic Publishers.
- Dannenber, M. P., & Wise, E. K. (2016). Seasonal climate signals from multiple tree ring metrics: A case study of *Pinus ponderosa* in the upper Columbia River Basin. *Journal of Geophysical Research: Biogeosciences*, *121*, 1178–1189. <https://doi.org/10.1002/2015JG003155>
- DeRose, R. J., Shaw, J. D., & Long, J. N. (2017). Building the forest inventory and analysis tree-ring data set. *Journal of Forestry*, *115*, 283–291. <https://doi.org/10.5849/jof.15-097>
- Dietze, M. (2017). *Ecological forecasting*. Princeton University Press.
- Dietze, M. C., Fox, A., Beck-Johnson, L. M., Betancourt, J. L., Hooten, M. B., Jarnevich, C. S., Keitt, T. H., Kenney, M. A., Laney, C. M., Larsen, L. G., Loescher, H. W., Lunch, C. K., Pijanowski, B. C., Randerson, J. T., Read, E. K., Tredennick, A. T., Vargas, R., Weathers, K. C., & White, E. P. (2018). Iterative near-term ecological forecasting: Needs, opportunities, and challenges. *Proceedings of the National Academy of Sciences of the United States of America*, *115*, 1424–1432. <https://doi.org/10.1073/pnas.1710231115>
- Domec, J.-C., Warren, J., Meinzer, F., Brooks, J., & Coulombe, R. (2004). Native root xylem embolism and stomatal closure in stands of Douglas-fir and ponderosa pine: mitigation by hydraulic redistribution. *Oecologia*, *141*, 7–16. <https://doi.org/10.1007/s00442-004-1621-4>
- Domke, G. M., Walters, B. F., Nowak, D. J., Smith, J., Ogle, S. M., Coulston, J. W., & Wirth, T. C. (2020). Greenhouse gas emissions and removals from forest land, woodlands, and urban trees in the United States, 1990–2018. <https://doi.org/10.2737/FS-RU-227>
- Dye, A., Plotkin, A. B., Bishop, D., Pederson, N., Poulter, B., & Hessl, A. (2016). Comparing tree-ring and permanent plot estimates of aboveground net primary production in three eastern U.S. forests. *Ecosphere*, *7*, e01454. <https://doi.org/10.1002/ecs2.1454>
- Ehle, D. S., & Baker, W. L. (2003). Disturbance and stand dynamics in ponderosa pine forests in Rocky Mountain National Park, USA. *Ecological Monographs*, *73*, 543–566. <https://doi.org/10.1890/03-4014>
- Evans, M. E. K., Falk, D. A., Arizpe, A., Swetnam, T. L., Babst, F., & Holsinger, K. E. (2017). Fusing tree-ring and forest inventory data to infer influences on tree growth. *Ecosphere*, *8*, e01889. <https://doi.org/10.1002/ecs2.1889>
- Fer, I., Kelly, R., Moorcroft, P. R., Richardson, A. D., Cowdery, E. M., & Dietze, M. C. (2018). Linking big models to big data: Efficient ecosystem model calibration through Bayesian model emulation. *Biogeosciences*, *15*, 5801–5830. <https://doi.org/10.5194/bg-15-5801-2018>
- Fernández-de-Uña, L., McDowell, N. G., Cañellas, I., & Gea-Izquierdo, G. (2016). Disentangling the effect of competition, CO₂ and climate on intrinsic water-use efficiency and tree growth. *Journal of Ecology*, *104*, 678–690. <https://doi.org/10.1111/1365-2745.12544>
- Ford, K. R., Breckheimer, I. K., Franklin, J. F., Freund, J. A., Kroiss, S. J., Larson, A. J., Theobald, E. J., & HilleRisLambers, J. (2016). Competition alters tree growth responses to climate at individual and stand scales. *Canadian Journal of Forest Research*, *47*, 53–62. <https://doi.org/10.1139/cjfr-2016-0188>
- Foster, J. R., Finley, A. O., D'Amato, A. W., Bradford, J. B., & Banerjee, S. (2016). Predicting tree biomass growth in the temperate-boreal ecotone: Is tree size, age, competition, or climate response most important? *Global Change Biology*, *22*, 2138–2151. <https://doi.org/10.1111/gcb.13208>
- Fox, A. M., Hoar, T. J., Anderson, J. L., Arellano, A. F., Smith, W. K., Litvak, M. E., MacBean, N., Schimel, D. S., & Moore, D. J. P. (2018).

- Evaluation of a data assimilation system for land surface models using CLM4.5. *Journal of Advances in Modeling Earth Systems*, 10, 2471–2494. <https://doi.org/10.1029/2018MS001362>
- Friedlingstein, P., Meinshausen, M., Arora, V. K., Jones, C. D., Anav, A., Liddicoat, S. K., & Knutti, R. (2013). Uncertainties in CMIP5 climate projections due to carbon cycle feedbacks. *Journal of Climate*, 27, 511–526. <https://doi.org/10.1175/JCLI-D-12-00579.1>
- Fritts, H. C., Smith, D. G., Cardis, J. W., & Budelsky, C. A. (1965). Tree-ring characteristics along a vegetation gradient in northern Arizona. *Ecology*, 46, 393–401. <https://doi.org/10.2307/1934872>
- Gatti, L. V., Basso, L. S., Miller, J. B., Gloor, M., Gatti Domingues, L., Cassol, H. L. G., Tejada, G., Aragão, L. E. O. C., Nobre, C., Peters, W., Marani, L., Arai, E., Sanches, A. H., Corrêa, S. M., Anderson, L., Von Randow, C., Correia, C. S. C., Crispim, S. P., & Neves, R. A. L. (2021). Amazonia as a carbon source linked to deforestation and climate change. *Nature*, 595, 388–393. <https://doi.org/10.1038/s41586-021-03629-6>
- Gelman, A., & Rubin, D. B. (1992). Inference from iterative simulation using multiple sequences. *Statistical Science*, 7, 457–472. <https://doi.org/10.1214/ss/1177011136>
- Grassi, G., House, J., Dentener, F., Federici, S., den Elzen, M., & Penman, J. (2017). The key role of forests in meeting climate targets requires science for credible mitigation. *Nature Climate Change*, 7, 220–226. <https://doi.org/10.1038/nclimate3227>
- Graumlich, L. J., Brubaker, L. B., & Grier, C. C. (1989). Long-term trends in forest net primary productivity: Cascade mountains, Washington. *Ecology*, 70, 405–410. <https://doi.org/10.2307/1937545>
- IPCC. (2014). *Climate change 2014: Synthesis report. Contribution of working groups I, II and III to the fifth assessment report of the Intergovernmental Panel on climate change*. IPCC.
- IPCC. (2018). *Global Warming of 1.5°C. An IPCC Special Report on the impacts of global warming of 1.5°C above pre-industrial levels and related global greenhouse gas emission pathways, in the context of strengthening the global response to the threat of climate change, sustainable development, and efforts to eradicate poverty*. Author.
- Itter, M. S., Finley, A. O., D'Amato, A. W., Foster, J. R., & Bradford, J. B. (2017). Variable effects of climate on forest growth in relation to climate extremes, disturbance, and forest dynamics. *Ecological Applications*, 27, 1082–1095. <https://doi.org/10.1002/eap.1518>
- Keane, R. E., Austin, M., Field, C., Huht, A., Lexer, M. J., Peters, D., Solomon, A., & Wyckoff, P. (2001). Tree mortality in gap models: Application to climate change. *Climatic Change*, 51, 509–540. <https://doi.org/10.1023/A:1012539409854>
- Klesse, S., DeRose, R. J., Guiterman, C. H., Lynch, A. M., O'Connor, C. D., Shaw, J. D., & Evans, M. E. K. (2018). Sampling bias overestimates climate change impacts on forest growth in the southwestern United States. *Nature Communications*, 9, 5336. <https://doi.org/10.1038/s41467-018-07800-y>
- Koch, G. W., Sillett, S. C., Jennings, G. M., & Davis, S. D. (2004). The limits to tree height. *Nature*, 428, 851–854. <https://doi.org/10.1038/nature02417>
- Koontz, M. J., Latimer, A. M., Mortenson, L. A., Fettig, C. J., & North, M. P. (2021). Cross-scale interaction of host tree size and climatic water deficit governs bark beetle-induced tree mortality. *Nature Communications*, 12, 129. <https://doi.org/10.1038/s41467-020-20455-y>
- Koven, C., Arora, V. K., Cadule, P., Fisher, R. A., Jones, C. D., Lawrence, D. M., Lewis, J., Lindsey, K., Mathesius, S., Meinshausen, M., Mills, M., Nicholls, Z., Sanderson, B. M., Swart, N. C., Wieder, W. R., & Zickfeld, K. (2021). 23rd Century surprises: Long-term dynamics of the climate and carbon cycle under both high and net negative emissions scenarios. *Earth System Dynamics*, 1–32. <https://doi.org/10.5194/esd-2021-23>
- Kunstler, G., Albert, C. H., Courbaud, B., Lavergne, S., Thuiller, W., Vieilledent, G., Zimmermann, N. E., & Coomes, D. A. (2010). Effects of competition on tree radial-growth vary in importance but not in intensity along climatic gradients. *Journal of Ecology*, 99, 300–312. <https://doi.org/10.1111/j.1365-2745.2010.01751.x>
- Lara, W., Bravo, F., & Maguire, D. A. (2013). Modeling patterns between drought and tree biomass growth from dendrochronological data: A multilevel approach. *Agricultural and Forest Meteorology*, 178–179, 140–151. <https://doi.org/10.1016/j.agrformet.2013.04.017>
- Lu, M., Zhou, X., Yang, Q., Li, H., Luo, Y., Fang, C., Chen, J., Yang, X., & Li, B. (2013). Responses of ecosystem carbon cycle to experimental warming: A meta-analysis. *Ecology*, 94, 726–738. <https://doi.org/10.1890/12-0279.1>
- Lundquist, J. E., & Negron, J. F. (2000). Endemic forest disturbances and stand structure of ponderosa pine (*Pinus ponderosa*) in the Upper Pine Creek Research Natural Area, South Dakota, USA. *Natural Areas Journal*, 20, 126–132.
- Luo, Y., Ogle, K., Tucker, C., Fei, S., Gao, C., LaDeau, S., Clark, J. S., & Schimel, D. S. (2011). Ecological forecasting and data assimilation in a data-rich era. *Ecological Applications*, 21, 1429–1442. <https://doi.org/10.1890/09-1275.1>
- McCullough, I. M., Davis, F. W., & Williams, A. P. (2017). A range of possibilities: Assessing geographic variation in climate sensitivity of ponderosa pine using tree rings. *Forest Ecology and Management*, 402, 223–233. <https://doi.org/10.1016/j.foreco.2017.07.025>
- McDowell, N. G., & Allen, C. D. (2015). Darcy's law predicts widespread forest mortality under climate warming. *Nature Climate Change*, 5, 669–672. <https://doi.org/10.1038/nclimate2641>
- McDowell, N. G., Williams, A. P., Xu, C., Pockman, W. T., Dickman, L. T., Sevanto, S., Pangle, R., Limousin, J., Plaut, J., Mackay, D. S., Ogee, J., Domec, J. C., Allen, C. D., Fisher, R. A., Jiang, X., Muss, J. D., Breshears, D. D., Rauscher, S. A., & Koven, C. (2016). Multi-scale predictions of massive conifer mortality due to chronic temperature rise. *Nature Climate Change*, 6, 295–300. <https://doi.org/10.1038/nclimate2873>
- McLeod, S. D., & Running, S. W. (2011). Comparing site quality indices and productivity in ponderosa pine stands of western Montana. *Canadian Journal of Forest Research*, 18(3), 346–352. <https://doi.org/10.1139/x88-052>
- Medlyn, B. E., Zaehle, S., De Kauwe, M. G., Walker, A. P., Dietze, M. C., Hanson, P. J., Hickler, T., Jain, A. K., Luo, Y., Parton, W., Prentice, I. C., Thornton, P. E., Wang, S., Wang, Y.-P., Weng, E., Iversen, C. M., McCarthy, H. R., Warren, J. M., Oren, R., & Norby, R. J. (2015). Using ecosystem experiments to improve vegetation models. *Nature Climate Change*, 5, 528–534. <https://doi.org/10.1038/nclimate2621>
- National Academies of Sciences, E. (2018). *Negative emissions technologies and reliable sequestration: A research agenda*. <https://doi.org/10.17226/25259>
- Ogle, K., Barber, J. J., Barron-Gafford, G. A., Bentley, L. P., Young, J. M., Huxman, T. E., Loik, M. E., & Tissue, D. T. (2015). Quantifying ecological memory in plant and ecosystem processes. *Ecology Letters*, 18, 221–235. <https://doi.org/10.1111/ele.12399>
- Pan, Y., Chen, J. M., Birdsey, R., McCullough, K., He, L., & Deng, F. (2011). Age structure and disturbance legacy of North American forests. *Biogeosciences*, 8, 715–732. <https://doi.org/10.5194/bg-8-715-2011>
- Parker, T. J., Clancy, K. M., & Mathiasen, R. L. (2006). Interactions among fire, insects and pathogens in coniferous forests of the interior western United States and Canada. *Agricultural and Forest Entomology*, 8, 167–189. <https://doi.org/10.1111/j.1461-9563.2006.00305.x>
- Peltier, D. M. P., & Ogle, K. (2019). Legacies of more frequent drought in ponderosa pine across the western United States. *Global Change Biology*, 25, 3803–3816. <https://doi.org/10.1111/gcb.14720>
- Peters, D. P. C., Pielke, R. A., Bestelmeyer, B. T., Allen, C. D., Munson-McGee, S., & Havstad, K. M. (2004). Cross-scale interactions, nonlinearities, and forecasting catastrophic events. *Proceedings of the National Academy of Sciences of the United States of America*, 101, 15130–15135. <https://doi.org/10.1073/pnas.0403822101>

- Plummer, M. (2019). *rjags: Bayesian graphical models using MCMC*. R package version 4-10. <https://CRAN.R-project.org/package=rjags>
- PRISM Climate Group, Oregon State University. (2004). <http://prism.oregonstate.edu>
- Rstudio Team. (2018). Rstudio: Integrated Development for R (version 1.2.1335). Boston, MA. <http://www.rstudio.com/>
- Reclamation. (2013). *Downscaled CMIP3 and CMIP5 climate and hydrology projections: Release of downscaled CMIP5 climate projections, comparison with preceding information, and summary of user needs*, prepared by the U.S. Department of the Interior, Bureau of Reclamation, Technical Services Center, Denver, Colorado. 47 pp.
- Schliep, E. M., Dong, T. Q., Gelfand, A. E., & Li, F. (2014). Modeling individual tree growth by fusing diameter tape and increment core data. *Environmetrics*, 25, 610–620. <https://doi.org/10.1002/env.2324>
- Shaw, J. D. (2000). Application of stand density index to irregularly structured stands. *Western Journal of Applied Forestry*, 15, 40–42. <https://doi.org/10.1093/wjaf/15.1.40>
- Shiklomanov, A. N., Bond-Lamberty, B., Atkins, J. W., & Gough, C. M. (2020). Structure and parameter uncertainty in centennial projections of forest community structure and carbon cycling. *Global Change Biology*, 26, 6080–6096. <https://doi.org/10.1111/gcb.15164>
- Smith, W. K., Fox, A. M., MacBean, N., Moore, D. J. P., & Parazoo, N. C. (2020). Constraining estimates of terrestrial carbon uptake: New opportunities using long-term satellite observations and data assimilation. *New Phytologist*, 225, 105–112. <https://doi.org/10.1111/nph.16055>
- Sohn, J. A., Saha, S., & Bauhus, J. (2016). Potential of forest thinning to mitigate drought stress: A meta-analysis. *Forest Ecology and Management*, 380, 261–273. <https://doi.org/10.1016/j.foreco.2016.07.046>
- Soranno, P. A., Cheruvilil, K. S., Bissell, E. G., Bremigan, M. T., Downing, J. A., Fergus, C. E., Filstrup, C. T., Henry, E. N., Lottig, N. R., Stanley, E. H., Stow, C. A., Tan, P.-N., Wagner, T., & Webster, K. E. (2014). Cross-scale interactions: Quantifying multi-scaled cause-effect relationships in macrosystems. *Frontiers in Ecology and the Environment*, 12, 65–73. <https://doi.org/10.1890/120366>
- Stout, D. L., & Sala, A. (2003). Xylem vulnerability to cavitation in *Pseudotsuga menziesii* and *Pinus ponderosa* from contrasting habitats. *Tree Physiology*, 23, 43–50. <https://doi.org/10.1093/treephys/23.1.43>
- Stovall, A. E. L., Shugart, H., & Yang, X. (2019). Tree height explains mortality risk during an intense drought. *Nature Communications*, 10, 4385. <https://doi.org/10.1038/s41467-019-12380-6>
- Swetnam, T., Allen, C. D., & Betancourt, J. L. (1999). Applied historical ecology: Using the past to manage for the future. *Ecological Applications*, 9, 1189–1206.
- Taylor, K. E., Stouffer, R. J., & Meehl, G. A. (2012). An overview of CMIP5 and the experiment design. *Bulletin of the American Meteorological Society*, 93, 485–498. <https://doi.org/10.1175/BAMS-D-11-00094.1>
- Thomas, R. Q., Brooks, E. B., Jersild, A. L., Ward, E. J., Wynne, R. H., Albaugh, T. J., Dinon-Aldridge, H., Burkhart, H. E., Domec, J.-C., Fox, T. R., Gonzalez-Benecke, C. A., Martin, T. A., Noormets, A., Sampson, D. A., & Teskey, R. O. (2017). Leveraging 35 years of *Pinus taeda* research in the southeastern US to constrain forest carbon cycle predictions: Regional data assimilation using ecosystem experiments. *Biogeosciences*, 14, 3525–3547. <https://doi.org/10.5194/bg-14-3525-2017>
- USDA Forest Service. (1999). *Forest survey field procedures*. USDA Forest Service, Interior West Resource Inventory, Monitoring, and Analysis Program.
- USDA Forest Service. (2015). *Forest Inventory and Analysis national core field guide. Vol I: Field data collection procedures for phase 2 plots, version 7.0*.
- Walker, A. P., Kauwe, M. G. D., Bastos, A., Belmecheri, S., Georgiou, K., Keeling, R. F., McMahon, S. M., Medlyn, B. E., Moore, D. J. P., Norby, R. J., Zaehle, S., Anderson-Teixeira, K. J., Battipaglia, G., Brienen, R. J. W., Cabugao, K. G., Cailleret, M., Campbell, E., Canadell, J. G., Ciais, P., ... Zuidema, P. A. (2020). Integrating the evidence for a terrestrial carbon sink caused by increasing atmospheric CO₂. *New Phytologist*. <https://doi.org/10.1111/nph.16866>
- Williams, A. P., Allen, C. D., Macalady, A. K., Griffin, D., Woodhouse, C. A., Meko, D. M., Swetnam, T. W., Rauscher, S. A., Seager, R., Grissino-Mayer, H. D., Dean, J. S., Cook, E. R., Gangodagamage, C., Cai, M., & McDowell, N. G. (2013). Temperature as a potent driver of regional forest drought stress and tree mortality. *Nature Climate Change*, 3, 292–297. <https://doi.org/10.1038/nclimate1693>
- Williams, A. P., Cook, E. R., Smerdon, J. E., Cook, B. I., Abatzoglou, J. T., Bolles, K., Baek, S. H., Badger, A. M., & Livneh, B. (2020). Large contribution from anthropogenic warming to an emerging North American megadrought. *Science*, 368, 314–318. <https://doi.org/10.1126/science.aaz9600>
- Zald, H. S. J., Spies, T. A., Harmon, M. E., & Twery, M. J. (2016). Forest carbon calculators: A review for managers, policymakers, and educators. *Journal of Forestry*, 114, 134–143. <https://doi.org/10.5849/jof.15-019>
- Zhang, J., Finley, K. A., Johnson, N. G., & Ritchie, M. W. (2019). Lowering stand density enhances resiliency of ponderosa pine forests to disturbances and climate change. *Forest Science*, 65, 496–507. <https://doi.org/10.1093/forsci/fxz006>
- Zhang, J., Oliver, W. W., & Busse, M. D. (2011). Growth and development of ponderosa pine on sites of contrasting productivities: Relative importance of stand density and shrub competition effects. *Canadian Journal of Forest Research*, 36(10), 2426–2438. <https://doi.org/10.1139/x06-078>
- Zipkin, E. F., Zylstra, E. R., Wright, A. D., Saunders, S. P., Finley, A. O., Dietze, M. C., Itter, M. S., & Tingley, M. W. (2021). Addressing data integration challenges to link ecological processes across scales. *Frontiers in Ecology and the Environment*, 19, 30–38. <https://doi.org/10.1002/fee.2290>

SUPPORTING INFORMATION

Additional supporting information may be found in the online version of the article at the publisher's website.

How to cite this article: Heilman, K. A., Dietze, M. C., Arizpe, A. A., Aragon, J., Gray, A., Shaw, J. D., Finley, A. O., Klesse, S., DeRose, R. J., & Evans, M. E. K. (2022). Ecological forecasting of tree growth: Regional fusion of tree-ring and forest inventory data to quantify drivers and characterize uncertainty. *Global Change Biology*, 00, 1–19. <https://doi.org/10.1111/gcb.16038>